



HAL
open science

Planar cell polarity regulators in asymmetric organogenesis during development and disease

De-Li Shi

► **To cite this version:**

De-Li Shi. Planar cell polarity regulators in asymmetric organogenesis during development and disease. JOURNAL OF GENETICS AND GENOMICS, 2022, 10.1016/j.jgg.2022.06.007 . hal-03719572

HAL Id: hal-03719572

<https://hal.sorbonne-universite.fr/hal-03719572v1>

Submitted on 11 Jul 2022

HAL is a multi-disciplinary open access archive for the deposit and dissemination of scientific research documents, whether they are published or not. The documents may come from teaching and research institutions in France or abroad, or from public or private research centers.

L'archive ouverte pluridisciplinaire **HAL**, est destinée au dépôt et à la diffusion de documents scientifiques de niveau recherche, publiés ou non, émanant des établissements d'enseignement et de recherche français ou étrangers, des laboratoires publics ou privés.

1 **Planar cell polarity regulators in asymmetric organogenesis during development**
2 **and disease**

3 De-Li Shi^{a,b,*}

4 ^aAffiliated Hospital of Guangdong Medical University, Zhanjiang 524001, China

5 ^bLaboratory of Developmental Biology, CNRS-UMR7622, Institut de Biologie Paris-Seine (IBPS),
6 Sorbonne University, 75005 Paris, France

7

8 *Correspondence: de-li.shi@upmc.fr

9

10 Running title: Asymmetry in organ morphogenesis

11

11 **Abstract**

12 The phenomenon of planar cell polarity is critically required for a myriad of morphogenetic
13 processes in metazoan and is accurately controlled by several conserved modules. Six “core”
14 proteins, including Frizzled, Flamingo (Celsr), Van Gogh (Vangl), Dishevelled, Prickle, and Diego
15 (Ankrd6), are major components of the Wnt/planar cell polarity pathway. The Fat/Dchs
16 protocadherins and the Scrib polarity complex also function to instruct cellular polarization. In
17 vertebrates, all these pathways are essential for tissue and organ morphogenesis, such as neural
18 tube closure, left-right symmetry breaking, heart and gut morphogenesis, lung and kidney
19 branching, stereociliary bundle orientation, and proximal-distal limb elongation. Mutations in
20 planar polarity genes are closely linked to various congenital diseases. Striking advances have
21 been made in deciphering their contribution to the establishment of spatially oriented pattern in
22 developing organs and the maintenance of tissue homeostasis. The challenge remains to clarify
23 the complex interplay of different polarity pathways in organogenesis and the link of cell polarity
24 to cell fate specification. Interdisciplinary approaches are also important to understand the roles
25 of mechanical forces in coupling cellular polarization and differentiation. This review outlines
26 current advances on planar polarity regulators in asymmetric organ formation, with the aim to
27 identify questions that deserve further investigation.

28 Key words: planar cell polarity, Wnt/PCP signaling, left-right asymmetry, heart and gut
29 morphogenesis, lung and kidney branching, inner ear hair cell orientation, limb outgrowth

30

30 Introduction

31 Planar cell polarity (PCP), initially studied in the retina and the wing of insects *Oncopeltus*
32 *fasciatus* and *Drosophila melanogaster* (Lawrence and Shelton, 1975; Gubb and García-Bellido,
33 1982), refers to coordinated cellular orientation within the plane of an epithelium or a tissue. This
34 fascinating process exerts wide functions in organizing the asymmetric cellular choreography and
35 the spatially oriented pattern during tissue and organ morphogenesis, contributing to, for
36 example, the architectural beauty of the *Drosophila* compound eye and the mammalian cochlea.
37 The phenomenon of PCP is mostly regulated by a set of evolutionarily conserved proteins,
38 including Frizzled receptors, Flamingo (Celsr1-3 in vertebrates), Dishevelled (Dvl1-3 in
39 vertebrates), Diego (Ankrd6 in vertebrates), Van Gogh (Vangl1-2 in vertebrates), and Prickle
40 (Prickle1-3 in vertebrates). These “core” PCP proteins transduce Wnt/PCP signaling to regulate
41 cytoskeletal rearrangements and polarized cell behaviors in a variety of morphogenetic
42 processes (Wallingford, 2012; Yang and Mlodzik, 2015; Henderson et al., 2018). Increasing
43 evidence suggests that several vertebrate Wnts, such as Wnt5a and Wnt11, are also important
44 components of the Wnt/PCP pathway, although they are not considered as “core” PCP proteins.

45 There are also other conserved protein complexes that function as important PCP
46 regulators in *Drosophila* and vertebrates. The heteromeric protocadherins Fat4 and Dchs1
47 (dachshous cadherin-related 1) represent the second PCP pathway (Fat/Dchs module) that is
48 regulated by the Golgi resident transmembrane kinase Four-jointed or Fj (Blair and McNeill,
49 2018). The Scrib (Scrb1 or Scribble1) polarity complex, originally identified as a regulator of
50 apico-basal cell polarity, consists of Scrib, Dlg (Discs-large) and Lgl (Lethal-giant larvae) proteins
51 (Milgrom-Hoffman and Humbert, 2018). These pathways exert broad activity in cellular signaling
52 and cytoskeletal organization. They function in concert with or independently of the “core”
53 Wnt/PCP pathway to regulate cell polarity. Two additional systems, the Fat2/Lar (leukocyte
54 antigen-related receptor tyrosine phosphatase) and Toll-8/Cirl (adhesion G protein-coupled
55 receptor) pathways, have been recently shown to instruct some *Drosophila* PCP processes, but
56 their functions in vertebrates merit future investigation (Lavalou and Lecuit, 2022).

57 The “core” PCP pathway, the Fat/Dchs polarity module and the Scrib complex are
58 critically involved in tissue and organ morphogenesis, from the emergence of organ primordia to
59 terminal organogenesis and tissue homeostasis. In vertebrates, the functions of PCP proteins
60 (herein collectively referred to as regulators of PCP-dependent cell behaviors) have been well
61 documented in many morphogenetic processes, such as neural tube closure, embryonic left-right
62 symmetry breaking, heart and gut morphogenesis, lung and kidney branching, orientation of inner
63 ear hair cells, and proximal-distal limb bud elongation (Yang and Mlodzik, 2015; Henderson et al.,
64 2018). Mutations of PCP genes impair organ development and are closely linked to various
65 congenital anomalies, including neural tube defects (Wang et al., 2019), laterality disorders
66 (Grimes and Burdine, 2017), hearing deficits (May-Simera and Kelley, 2012), lung and kidney
67 diseases (Vladar and Königshoff, 2020; Torban and Sokol, 2021), as well as limb abnormalities
68 (Gao and Yang, 2013). Importantly, PCP proteins regulate common cellular processes underlying
69 the outgrowth and elongation of tissue primordia, such as convergent extension (CE) movements
70 driven by oriented cell division and intercalation (Wallingford, 2012). Therefore, their dysfunctions
71 can lead to multiple phenotypes, highlighting a general importance in organogenesis. There are
72 many excellent reviews focusing on PCP functions in specific aspects of morphogenesis, but a
73 more comprehensive analysis of PCP regulators during development of different organs that
74 display PCP-dependent cellular organization is beneficial for understanding their complex
75 interplay in the establishment of cell polarity. This review attempts to present past achievements
76 and latest advances of PCP protein functions in asymmetric organogenesis, with the aim to
77 identify challenges in deciphering the extraordinary process of asymmetry formation.

78 **Wnt signaling pathways and planar cell polarity protein complexes**

79 Vertebrate Wnt pathways can be divided into three branches based on the activation of
80 different biological readouts (Fig. 1A). Wnt/ β -catenin or canonical Wnt signaling induces target
81 gene transcription and cell fate specification by stabilizing β -catenin through inhibition of its
82 destruction complex. Non-canonical Wnt signaling includes Wnt/PCP and Wnt/ Ca^{2+} branches that
83 function independently of β -catenin. Wnt/PCP signaling controls cell polarity by regulating
84 cytoskeletal rearrangements and/or transcriptional responses. It functions through several well-

85 characterized planar polarity effector (PPE) proteins, such as Daam1 (Dishevelled-associated
86 activator of morphogenesis 1), Rho family of small GTPases and Jun N-terminal kinase (JNK),
87 but also via a few less well-studied ciliogenesis and planar polarity effector (CPLANE) proteins
88 including Intu, Fuz and Wdpcp (Adler and Wallingford, 2017). Wnt/Ca²⁺ signaling triggers
89 intracellular calcium flux to induce actin polymerization and NFAT (nuclear factor of activated T-
90 cells)-mediated target gene transcription. Dvl family proteins function in all Wnt pathway branches
91 through distinct domains including DIX, PDZ and DEP (Shi, 2020). Their conserved C-terminus
92 PDZ domain-binding motif can modulate Wnt/ β -catenin and Wnt/PCP signaling through
93 interaction with the PDZ domain (Lee et al., 2015).

94 The “core” PCP proteins form two separate complexes that are distributed on opposite
95 cell borders within the tissue plane (Fig. 1B,C). Frizzled (Fzd), Dvl and Ankrd6 reside on one side
96 of the cell, while Vangl and Prickle localize to the opposite side. Celsr is present on both sides
97 and forms homodimers between adjacent cells to propagate polarity information across cells.
98 This asymmetric distribution of “core” PCP proteins is a hallmark of planar polarization and
99 reflects the coordinated cellular orientation during tissue or organ morphogenesis. Vertebrate
100 Wnt5a signaling gradient can provide global cues to instruct the asymmetric localization of “core”
101 PCP proteins in several well-documented PCP-dependent processes, such as the proximal-distal
102 development of limb bud and the anteroposterior (AP) polarization of node cells (Gao et al., 2011;
103 Minegishi et al., 2017). Similarly, Fat and Dchs heteromeric protocadherins are localized to
104 opposite sides of adjacent cells (Fig. 1B), and they may function either as a ligand or as a
105 receptor for the other to mediate cell interaction (Blair and McNeill, 2018). Through a multitude of
106 biochemical, functional and genetic interactions, PCP proteins regulate non-canonical Wnt
107 signaling and make an important contribution to the spatiotemporal organization of cellular
108 activities in a variety of tissues and organs (Table 1). The following sections will detail their
109 implications in asymmetric organ morphogenesis during development and disease.

110 **Early embryonic left-right asymmetry**

111 Left-right asymmetry, either external or internal, is a common feature in animals. Although
112 vertebrate embryos are seemingly symmetrical, they already display asymmetric gene expression

113 at early stages of development. This is critical for the asymmetric formation of internal organ
114 primordia and their subsequent morphogenesis to generate left-right differences in sizes, shapes
115 and anatomical locations. Transient structures formed during early development, such as the
116 posterior gastrocoel roof plate (GRP) in *Xenopus*, the Kupffer's vesicle (KV) in zebrafish, the
117 Hensen's node in chick and the node in mice, constitute the left-right organizer (LRO) involved in
118 breaking the bilateral symmetry across the mediolateral plane (Fig. 2A,B). They initiate left-right
119 asymmetry by providing instructive signals mostly through cilia-mediated directional fluid flow
120 (Axelrod, 2020; Little and Norris, 2021). Wnt/PCP signaling acts in the LRO to coordinate the
121 orientation of individual cells and multicellular structures with respect to the embryonic axes.
122 Subsequently, signals generated in a manner that is both dependent and independent on motile
123 cilia create a gradient of Nodal protein to activate left-sided expression of the Nodal-Lefty-Pitx2
124 network (Grimes and Burdine, 2017; Axelrod, 2020). Thus, differential gene activation and
125 repression establish left-right embryonic polarity that will influence the asymmetric
126 morphogenesis of organ primordia.

127 Dvl, Vangl and Prickle are important for cilia-dependent asymmetric fluid flow. In node
128 cells, Vangl1, Vangl2 and Prickle2 are localized to the anterior side, while Dvl2 and Dvl3 are
129 enriched at the posterior side (Antic et al. 2010; Hashimoto et al., 2010; Grimes and Burdine,
130 2017). Wnt5a and Wnt5b, which are expressed posteriorly relative to the node, form a diffusible
131 gradient and provide instructive signals to induce the asymmetric localization of Vangl1 and
132 Prickle2, thus polarizing node cells along the AP axis (Minegishi et al., 2017). The asymmetric
133 localization of "core" PCP proteins then restricts the posterior positioning of ciliary basal bodies at
134 the dome-shaped apical surfaces of node cells and promotes the posterior tilting of cilia by
135 coordinating the asymmetric distribution of microtubules and actomyosin networks (Sai et al.,
136 2022). Subsequently, cilia-driven leftward fluid flow across the node initiates left-right asymmetry.
137 Knockout of Dvl2 and Dvl3 impairs the posterior location of ciliary basal bodies (Hashimoto et al.,
138 2010). Loss of Vangl1 and Vang2 disrupts the posterior orientation of primary motile cilia in the
139 LRO, resulting in defective expression of Nodal and Pitx2 on the left side (Borovina et al., 2010;
140 Antic et al., 2010; Song et al., 2010). Consistent with their association into a complex, Prickle1

141 and Prickle2 interact with Vangl2 to regulate its anterior localization in node cells (Minegishi et al.,
142 2017), while Prickle3 shows reciprocal interactions with Vangl2 for the anterior localization in
143 GRP cells to promote growth and posterior positioning of motile cilia (Chu et al., 2016).
144 Downstream of “core” PCP proteins, JNK activity is required for modulating ciliogenesis and cilia
145 length in the zebrafish KV (Derrick et al., 2022). Altogether, these observations reveal an
146 important implication of Wnt/PCP signaling in the orientation of motile cilia within the LRO. Thus,
147 the AP polarity generated by the asymmetric distribution of PCP proteins can be translated into
148 left-right asymmetry through the directional fluid flow.

149 The unconventional Myosin1D (Myo1D) also functions to shape the cilia-driven directional
150 fluid flow in the LRO, although unlikely being a component of the Wnt/PCP pathway. It interacts
151 with Vangl2 to initiate left-right axis formation in zebrafish and *Xenopus* embryos (Juan et al.,
152 2018; Tingler et al., 2018). In the zebrafish KV, Myo1D antagonizes the activity of Vangl2 to
153 restrict the localization of posteriorly pointing cilia at the anterior region and anteriorly pointing
154 cilia at the posterior region, thereby establishing a circular geometry of fluid flow (Juan et al.,
155 2018). Thus, the cilia-dependent function of Myo1D acts in concert with Wnt/PCP signaling to
156 break left-right symmetry.

157 **Asymmetric cardiac morphogenesis**

158 The rightward looping of the heart primordium contributes to determine the relative
159 position of cardiac chambers and is the first event of asymmetric organogenesis (Desgrange et
160 al., 2018). It is initiated by the transformation of the cardiac tube into a loop (Fig. 2C). Abnormal
161 left-right patterning is intimately associated with congenital heart diseases, such as X-linked
162 heterotaxy caused by mutations of the ZIC3 transcription factor. Recent evidence suggests that
163 Zic3 regulates the expression of PCP genes and is required for Dvl phosphorylation during node
164 morphogenesis. It also genetically interacts with PCP genes to establish the left-right heart
165 asymmetry (Bellchambers and Ware, 2021). Therefore, there is a possibility that dysregulation of
166 PCP proteins may represent an underlying mechanism of ZIC3 mutations in congenital disorders
167 associated with heterotaxy.

168 Wnt/PCP signaling critically regulates heart morphogenesis after looping, particularly
169 directional cell movements from the second heart field (SHF) during outflow tract (OFT)
170 development (Henderson et al., 2006). Wnt5a, Wnt5b and Wnt11 are important for modulating
171 extracellular matrix composition, cytoskeletal rearrangements, actomyosin contractility, and cell
172 adhesion during SHF deployment and heart tube remodeling (Zhou et al., 2007; Sinha et al.,
173 2015; Merks et al., 2018). Loss of Wnt5a in mice leads to OFT malformations due to impaired cell
174 deployment in the SHF (Sinha et al., 2015). Moreover, Wnt5a functions through Daam1 in OFT
175 morphogenesis by promoting the AP elongation of the SHF (Li et al., 2019).

176 Dvl family members collectively contribute to OFT morphogenesis. Loss of Dvl1 and Dvl2
177 impairs SHF deployment and OFT lengthening by disrupting actin polymerization and filopodia
178 formation (Sinha et al., 2012). Homozygous *Looptail* mice, which carry a single nucleotide
179 mutation in the *Vangl2* gene that is predicted to produce a malfunctional Vangl2 protein, show
180 defects in the polarization of myocardial cells likely due to reduced activity of RhoA and ROCK1
181 (Rho-associated kinase 1). As a consequence, myocardializing cells fail to extend cellular
182 protrusions into the OFT cushion, resulting in abnormal muscularization of the proximal outlet
183 septum (Phillips et al., 2005). Conditional knockout of Vangl2 indicates that it is solely required
184 within the SHF to promote lengthening of the OFT by regulating cellular polarity in the distal
185 outflow wall (Ramsbottom et al., 2014). Similarly, loss of Prickle1 in mice leads to shortened OFT
186 due to absence of polarized cell orientation in the SHF (Gibbs et al., 2016). Conditional knockout
187 of Daam1 in the myocardium prevents cardiomyocytes from extending protrusions into the OFT
188 (Ajima et al., 2015). Disruption of the CPLANE protein Wdpcp in mice also prevents polarized
189 migration of cardiomyocytes to invade the OFT cushion and causes OFT septation defects (Cui
190 et al., 2013). Thus, Wnt/PCP signaling coordinates directional cell migration in the SHF to
191 promote heart morphogenesis.

192 PCP proteins are also involved in other aspects of heart development. In mice, Fzd4 is
193 required for arterial and arteriolar formation. It cooperates with Dvl3 to regulate vascular cell
194 proliferation and migration through microtubule stabilization and cellular polarization (Descamps
195 et al., 2012). Fzd2 and Fzd7 are redundantly required for CE movements to promote closure of

196 the ventricular septum (Yu et al., 2012). Vangl2 interacts with RhoA and ROCK in the formation
197 of the coronary vasculature through a non-autonomous manner, likely by regulating deposition of
198 fibronectin in the subepicardial space for the migration of epicardially-derived cells (Phillips et al.,
199 2008). Combined loss of Daam1 and Daam2 in mice causes severe cardiac abnormalities
200 including ventricular noncompaction, ventricular septal defects, irregular sarcomere assembly,
201 and impaired myocardial maturation (Li et al., 2011; Ajima et al., 2015). However, it is unclear
202 whether these defects are all direct consequences of disrupted Wnt/PCP signaling.

203 **Gut looping and elongation**

204 The left-right asymmetry of the developing gut arises through an important morphogenetic
205 process known as gut looping. This event has been shown to rely on physical forces generated
206 by differential growth rates between the gut and the dorsal mesentery that connects the gut to the
207 body wall (Savin et al., 2011). The earliest left-right asymmetric gut morphology is manifested by
208 the leftward curvature of the stomach (Fig. 2D). In the chick embryo, Nodal-induced expression of
209 Pitx2 maintains left-side identity of the early gut tube (Huycke and Tabin, 2018; Grzymkowski et
210 al., 2020). Wnt/PCP signaling acts downstream of Pitx2 to coordinate asymmetric processes of
211 the digestive system, including gut looping, intestine elongation, villification of the intestinal
212 epithelium, stem cell lineage segregation, and maintenance of epithelial homeostasis.

213 Several PCP proteins display asymmetric expression in the chicken dorsal mesentery,
214 which exhibits polarized cellular behaviors with extensive membrane contacts between adjacent
215 mesenchymal cells on the left side. Fzd4 and Daam2 show Pitx2-dependent left-sided
216 expression, and Daam2 is required for cell adhesion necessary for mesenchymal condensation in
217 the dorsal mesentery (Welsh et al., 2013). Although Wnt5a does not display asymmetric
218 expression, its activity on the right side is antagonized by the right-sided expression of secreted
219 Frizzled-related proteins (sFRPs). Therefore, the asymmetric activation of Wnt5a-Fzd4-Daam2
220 pathway triggers leftward tilt of the midgut (Welsh et al., 2013).

221 Intestine elongation critically requires functional PCP signaling. In mice, Wnt5a is
222 expressed in the gut mesenchyme. Constitutive knockout of Wnt5a disrupts midgut elongation by
223 preventing post-mitotic daughter cells from re-intercalating into the epithelial layer (Cervantes et

224 al., 2009) as well as from extending filopodia for basal return of their nuclei during interkinetic
225 nuclear migration (Wang et al., 2018). Ror2 and Ryk differentially regulate midgut elongation
226 through dynamic spatiotemporal interactions with Wnt5a. Mesenchyme-derived Ror2 functions
227 before the early phase of midgut elongation, while both epithelial and mesenchymal Ryk
228 contributes to midgut elongation throughout the early phase (Wang et al., 2020). Vangl2
229 regulates several polarized cell behaviors in the gut epithelium to couple epithelial
230 morphogenesis with gut tube elongation. In mice, it functions with Wnt5a for oriented cell division
231 along the rostrocaudal axis to increase fore-stomach length (Matsuyama et al., 2009). In
232 *Xenopus*, Vangl2 is enriched at the apical and anterior surfaces of radially elongated gut
233 endoderm cells; it coordinates microtubule organization, cell adhesion and endodermal cell shape
234 changes to promote gut elongation and lumen formation (Dush and Nascone-Yoder, 2019). At
235 late stages of intestine elongation, the Fat4/Dchs1 module acts in parallel with Vangl2 to drive
236 mesenchymal cell clustering necessary for epithelial folding during villus formation, while Wnt5a
237 functions upstream of Fat4 and acts as a chemoattractant to guide directional migration of
238 mesenchymal cells (Rao-Bhatia et al., 2020).

239 The gene encoding cilia and flagella associated protein 126, *Cfap126* (also known as
240 *Flattop* or *Fltp*), is transcriptionally activated during Wnt/PCP acquisition in ciliated cells, thus
241 representing a target of Wnt/PCP signaling (Gegg et al., 2014). *Cfap126* can function as a PPE,
242 and its transient expression in *Lgr5*⁺ intestinal stem cells regulates lineage priming and cell cycle
243 exit at the base of the crypt, contributing to the differentiation of Paneth and enteroendocrine cells
244 (Böttcher et al., 2021). In the adult, Wnt5a is expressed in *FoxL1*⁺ telocytes at the crypt-villus
245 junction regions and is required for homeostatic renewal of the intestinal epithelium (Shoshkes-
246 Carmel et al., 2018). These data highlight an essential role of Wnt/PCP signaling in intestinal
247 stem cell lineage segregation and directly link cell polarity to cell fate specification.

248 **Lung branching morphogenesis**

249 The highly elaborated and polarized architecture of the respiratory system emerges from
250 reciprocal interactions between lung epithelium and mesenchyme (Fig. 3A). Lung branching
251 morphogenesis involves repetitive formation of new buds, epithelial sprouting, and tube

252 elongation to generate an arborized airway network. This process is also dependent on several
253 aforementioned asymmetric cell behaviors. PCP proteins regulate different aspects of lung
254 morphogenesis, and their dysfunctions are linked to lung diseases, such as emphysema, a
255 chronic obstructive pulmonary disease, also known as COPD (Vladar and Königshoff, 2020).

256 In the mouse embryo, *Wnt5a* is mainly expressed in the mesenchyme of branch points
257 and functions through *Ror2* to synchronize radial polarization of mesenchymal cells for tube
258 elongation along the AP axis (Kishimoto et al., 2018). It also activates the *Ror2-Vangl2* cascade
259 in both lung epithelium and mesenchyme to coordinate alveolar formation through cytoskeleton-
260 mediated cell shape changes of alveolar type I cells and migration of myofibroblasts. Moreover,
261 *Wnt5a* and *Vangl2* show reduced expression in lung tissues of human patients with
262 bronchopulmonary dysplasia and emphysema, suggesting a possible implication of these genes
263 in lung diseases (Li et al., 2020; Zhang et al., 2020). *Fzd2* regulates epithelial cell shape changes
264 to promote branch point formation through RhoA-induced apical localization of phosphorylated
265 myosin light chain 2 (Kadzic et al., 2014). *Celsr1* and *Vangl2* are enriched at the basal/luminal
266 surface of branching lung epithelial buds. They regulate cytoskeletal remodeling likely via ROCK
267 to maintain epithelial architecture, thus their mutations lead to a reduced number of epithelial
268 branches (Yates et al., 2010b). Tracheal and alveolar epithelial cells from heterozygous *Looptail*
269 mice show highly disrupted actomyosin networks and abnormal focal adhesions, which are
270 correlated with decreased RhoA activity and reduced YAP signaling, suggesting that *Vangl2* may
271 function as a regulator of mechanotransduction (Cheong et al., 2020). *Scrib* is required for lumen
272 morphogenesis. It maintains tight junction integrity and epithelial cohesion through interaction
273 with Wnt/PCP signaling by modulating the localization of *Celsr1* and *Vangl2* in lung epithelium
274 (Yates et al., 2013).

275 Airway motile cilia present distinct orientations and highly coordinated movements, which
276 are important for mucociliary clearance. During ciliogenesis, asymmetrically localized PCP
277 complexes first polarize epithelial cells along the proximal (oral) to distal axis, and then provide
278 polarity cues to orient ciliary basal bodies in the proximal direction (Vladar et al., 2016). In airway
279 epithelia, *Fzd3*, *Fzd6*, *Dvl1* and *Dvl3* are enriched at the proximal side of multiciliated cells;

280 Vangl1, Vangl2 and Prickle2 are distributed at the distal side (Vladar et al., 2012, 2016); Dvl2 and
281 Ankrd6 are localized to the base of cilia (Vladar et al., 2012). Loss of PCP protein expression or
282 localization leads to mis-orientations of airway cilia and chronic inflammatory lung diseases
283 (Vladar et al., 2012, 2016), suggesting an essential role of PCP signaling in maintaining lung
284 homeostasis during fetal and post-natal development. Indeed, conditional knockout of Vangl1 or
285 Prickle2 in mice impairs tracheal epithelial regeneration (Vladar et al., 2016); reducing the activity
286 of Vangl2 causes tissue damage as observed in emphysema and impairs adult lung function
287 (Poobalasingam et al., 2017). Knockout of Cfap126 mostly reduces the diameter of terminal lung
288 bronchioles, leading to constricted distal airways in the post-natal lung (Gegg et al., 2014).

289 Wnt/PCP signaling also coordinates the development of pulmonary airway and
290 vasculature. Wnt5a interacts with Ror2 to direct avian pulmonary vasculogenesis by regulating
291 VEGF signaling through fibronectin expression in the mesenchyme (Loscertales et al., 2008).
292 Pericytes are perivascular cells that promote vessel maturation. Loss of Wnt5a and Fzd7 impairs
293 endothelium-pericyte interactions during pulmonary angiogenesis by disrupting the motility and
294 polarity of pericytes, which may contribute to pulmonary arterial hypertension (Yuan et al., 2019).
295 Since PCP proteins are critically involved in lung development, homeostasis and disease, it will
296 be important to further decipher the mechanisms by which they orchestrate stage-specific cellular
297 activities, ranging from epithelial-mesenchymal interactions in branching morphogenesis to the
298 maturation of multiciliated cells and the development of respiratory vasculature.

299 **Kidney development**

300 The morphogenesis of the early urinary tract involves reciprocal interactions between the
301 Wolffian duct-derived ureteric bud and its adjacent metanephric mesenchyme. Strikingly, the
302 ureteric bud undergoes reiterative branching morphogenesis with distal elements engaged in
303 directed cell migration, oriented cell division, and cell intercalation. These PCP-dependent cellular
304 behaviors play important roles in ureteric bud branching, tubular elongation, and tubule diameter
305 establishment (Carroll and Yu, 2012). Different polarity pathways are critically implicated in
306 kidney development and potentially linked to various genetic disorders, such as congenital

307 malformations of the kidney and urinary tract (CAKUT) and glomerular diseases (Torban and
308 Sokol, 2021).

309 It is well documented that Wnt ligands are essential in kidney morphogenesis. Pioneer
310 studies have demonstrated a requirement of Wnt4 for mesenchymal to epithelial transformation
311 that results in epithelialization of the ureteric bud (Stark et al., 1994; Kispert et al., 1998). Wnt5a-
312 Ror2 signaling regulates epithelial tubular formation from the ureteric bud. Loss of Wnt5a or Ror2
313 in mice impairs the positioning of metanephric mesenchyme and causes its aberrant interaction
314 with the Wolffian duct, resulting in duplicated ureters and kidneys (Nishita et al., 2014; Yun et al.,
315 2014). Wnt9b acts through Rho/JNK signaling to regulate CE movements and maintain polarized
316 cell divisions in the epithelium during early stages of kidney morphogenesis, thus inhibition of
317 Wnt9b-mediated signaling affects epithelial polarity and causes increased tubule diameter
318 (Karner et al., 2009). Wnt11 derived from the ureteric branch tip promotes the stable attachment
319 of nephron progenitors to the epithelial tip by regulating their polarity and motile behaviors,
320 thereby maintaining nephrogenic niche integrity (O'Brien et al., 2018).

321 Several “core” PCP proteins clearly display asymmetric localization in developing renal
322 tubule epithelia along the proximal-distal axis. In both the collecting duct and proximal tubules,
323 Vangl1 and Vangl2 are accumulated at the proximal side, while Fzd3 and Fzd6 are distributed at
324 the distal side, suggesting that they are involved in the polarization of renal tubules (Kunimoto et
325 al., 2017). Functional analyses indicate that other “core” PCP proteins are also important for renal
326 tubule morphogenesis. Mice deficient for Fzd4 and Fzd8 show renal hypoplasia, with delayed
327 growth, branching and proliferation of the ureteric epithelium (Ye et al., 2011). However, these
328 phenotypes may also result from disrupted Wnt/ β -catenin signaling. Perturbation of Dvl function
329 in *Xenopus* disrupts rosette-based CE movements driven by mediolaterally oriented cell
330 intercalations, resulting in shorter and wider kidney tubules (Lienkamp et al., 2012). Vangl2
331 regulates morphogenetic processes in the ureteric bud and metanephric mesenchyme.
332 Homozygous *Looptail* mice show defective ureteric branching and glomerular maturation but with
333 normal ureteric bud formation, consistent with impaired CE movements (Yates et al., 2010a).
334 Prickle1 is required for tubule morphogenesis by regulating the distribution of actin cytoskeleton

335 in the ureteric bud; its loss of function impairs cell arrangements in the collecting duct and renal
336 tubules, resulting in abnormal tubule shape (Liu et al., 2014). *Celsr1* genetically interacts with
337 *Vangl2* to regulate rostrocaudal patterning of renal tubules and maturation of glomeruli; it also
338 promotes ureteric tree growth during early stages of kidney development but prevents tubule
339 overgrowth at late stages (Brzóška et al., 2016). Consistent with these functions, mutations of
340 *CELSR1* are associated with renal disorders, including unilateral renal agenesis, hydronephrosis,
341 and hydroureter (Brzóška et al., 2016). Therefore, it will be important to understand the molecular
342 and cellular mechanisms underlying the stage-specific functions of *Celsr1* in kidney development.

343 Effectors of Wnt/PCP signaling are implicated in different aspects of renal tubule
344 development. In *Xenopus* and zebrafish pronephros, *Daam1* may function through Rho GTPase
345 to regulate cytoskeletal rearrangements for proper tubulogenesis and tubule morphology (Miller
346 et al., 2011). It also colocalizes with E-cadherin at cell-cell contact regions in the *Xenopus* nephric
347 primordium to ensure intercellular adhesion and epithelial tissue organization during CE
348 movements (Krneta-Stankic et al., 2021). In mice, *Fuz* appears to regulate ureteric bud branching
349 morphogenesis through cilia-dependent and -independent pathways, raising the possibility that it
350 may play a role in ciliogenesis (Wang et al., 2021).

351 *Fat* and *Dchs* heteromeric protocadherins are important for cell interactions in the
352 developing kidney. Loss of *Fat4* disrupts polarized cell behaviors and leads to cyst formation
353 (Saburi et al., 2008). *Fat1* cooperates with *Fat4* in renal tubular elongation (Saburi et al., 2012).
354 Importantly, the interaction between *Fat4* and *Dchs1* is necessary for ureteric bud branching and
355 tubule diameter establishment. *Dchs1* is specifically expressed in the cap (condensing)
356 mesenchyme that coalesces around the ureteric bud, while *Fat4* is only present in stromal cells
357 that surround the cap mesenchyme (Fig. 3B). These expression patterns establish a crosstalk
358 whereby *Fat4* interacts with *Dchs1* to regulate self-renewal and differentiation of ureteric epithelial
359 progenitors through Hippo, Notch or FGF signaling (Das et al., 2013; Bagherie-Lachidan et al.,
360 2015). *Fat4/Dchs1*-mediated stroma-to-cap signaling may also function to polarize the cap
361 mesenchyme for proper nephrogenesis (Mao et al., 2015). There is also a complex interplay
362 between *Fat* family protocadherins and other signaling pathways during kidney development. In

363 zebrafish pronephros, Fat1 functions with Scrib in Hippo signaling through regulation of YAP1.
364 Depletion of Fat1 and Scrib causes severe cyst formation, suggesting that Scrib may couple Fat1
365 with the Hippo pathway to coordinate cellular polarization and growth (Skouloudaki et al., 2009).
366 In mice, Fat4 can act non-autonomously to prevent ectopic ureteric bud formation and kidney
367 duplication by fine-tuning the signaling function of nephric duct-expressed RET, a GDNF receptor
368 that regulates cell rearrangements in ureteric bud morphogenesis (Zhang et al., 2019). Thus,
369 Fat4 plays a critical role in the cap mesenchyme to control the nephron progenitor pool.

370 Wnt/PCP signaling is also important for proper organization of podocytes, which are highly
371 specialized and polarized glomerular visceral epithelial cells that are essential for maintaining the
372 correct function of the glomerular filtration barrier to prevent proteinuria. Podocyte-specific loss of
373 Vangl2 in mice causes abnormal glomerular maturation in fetal kidneys and increases the
374 susceptibility of glomerular injury in the adults (Rocque et al., 2015). Thus, Vangl2 play an
375 important role to promote glomerular development and protect glomerular injury.

376 The improved understanding of PCP proteins in kidney morphogenesis helps to clarify the
377 link between Wnt/PCP signaling and chronic kidney failure. Nephron, the functional unit of the
378 kidney, uses numerous ciliated epithelial tubules to reabsorb nutrients and concentrate waste
379 products. Dysfunctions of primary cilia contribute to the pathogenesis of polycystic kidney disease
380 (PKD). As Wnt/PCP signaling, PKD genes encoding proteins mainly localized to primary cilia are
381 also required for oriented cell divisions and CE movements in developing renal tubules, inferring
382 that defective Wnt/PCP signaling may contribute to PKD as well. However, recent studies
383 indicate that mutations of PKD genes disrupt renal tubule morphogenesis independently of
384 Wnt/PCP signaling and that the asymmetric localization of PCP proteins remains intact in adult
385 cystic kidney (Kunimoto et al., 2017). Moreover, collecting duct-specific loss of Vangl1 and
386 Vangl2 in mice impairs oriented cell divisions and CE movements, leading to abnormal tubule
387 diameter in pre-natal renal tubules but not cyst formation in post-natal development (Kunimoto et
388 al., 2017; Derish et al., 2020). Therefore, PCP proteins play an important role in the accurate
389 control of tubule lumen diameter. Nevertheless, it remains to be determined in more detail how

390 they regulate early and late stages of kidney epithelial morphogenesis and how they are linked to
391 other kidney diseases.

392 **Inner ear development and hair cell polarity**

393 The inner ear exhibits marvelous features of PCP-dependent asymmetric morphogenesis,
394 making it an attractive system for studying PCP regulation and function. Mammalian inner ear
395 consists of a snail-shaped cochlea required for hearing and a vestibular system necessary for
396 maintaining balance. Cochlear extension and development of the spiral organ of Corti from a
397 thicker and shorter primordium involve cell intercalations at the luminal surface and directed
398 migration of hair cells toward the apex (Driver et al., 2017). These highly regulated cellular
399 processes promote cochlea growth and contribute to the spatial distribution of sensory cells.
400 Thus, the organ of Corti forms one row of inner hair cells (IHCs) and three rows of outer hair cells
401 (OHC1, OHC2, and OHC3), which are separated by specialized supporting cells. Based on their
402 locations with respect to the center of the cochlear spiral, IHCs are referred to as neural/medial
403 (or proximal), while OHCs are described as abneural/lateral (or distal). Strikingly, both cochlear
404 and vestibular hair cells display uniformly oriented stereociliary bundles on their apical surfaces.
405 Wnt/PCP signaling functions to promote cochlea growth and organize the highly choreographed
406 orientation of stereociliary bundles.

407 In cochlear and vestibular epithelia of the developing mouse embryo, PCP proteins
408 display striking asymmetric localization in both sensory and supporting cells in a pattern that is
409 tightly linked to hair cell polarity (Fig. 4A). Fzd3, Fzd6 and Dvl1 accumulate at the neural
410 boundary of IHCs and OHCs, opposite to the site of stereociliary bundle formation, while Dvl2
411 and Dvl3 are apparently enriched at the abneural edge (Najarro et al., 2020). Ankrd6 localizes to
412 the neural edge (Jones et al., 2014). Celsr1 is likely enriched both at the neural side of hair cells
413 and at the abneural side of supporting cells (Duncan et al., 2017). Analysis by stimulated
414 emission depletion microscopy indicates that Vangl2 is present at the abneural side of supporting
415 cells (Giese et al., 2012). Prickle2 is enriched at the neural side of vestibular hair cells before the
416 formation of stereocilia, and Vangl2 maintains this asymmetric distribution (Deans et al., 2007).

417 Dysfunctions of PCP proteins affect cochlear outgrowth and hair cell polarity. Wnt5a alone
418 is not sufficient for hair cell polarization in the developing cochlea, but multiple Wnt ligands
419 collectively contribute to this process (Najarro et al., 2020). During cochlear extension to form the
420 organ of Corti, Dvl1, Dvl2 and Vangl2 regulate cell intercalation that drives unidirectional
421 elongation of the primordium. Loss of their functions interferes with outgrowth and
422 morphogenesis of the cochlea, resulting in abnormal patterning of the cochlear duct and defective
423 uniform hair bundle orientation (Montcouquiol et al., 2003; Wang et al., 2005). Combined loss of
424 Fzd3 and Fzd6 mostly affects hair bundle orientation in the organ of Corti (Wang et al., 2006). In
425 mice, missense mutations that may reduce the structural integrity of Celsr1 protein disrupt the
426 earliest stages of hair cell polarity in the cochlea and lead to mis-oriented stereociliary bundles
427 between vestibular hair cells associated with defective vestibular behaviors (Curtin et al., 2003).
428 Knockout of Fat4 mildly affects hair bundle orientation by mostly leads to defects in cochlear
429 extension and organization of OHCs, which are exacerbated by reducing the dosage of Fat1
430 (Saburi et al., 2012).

431 Different PCP genes show genetic interactions in cochlear extension and stereociliary
432 bundle orientation, likely due to functional redundancy and interdependent asymmetric
433 localization of their protein products. In particular, there is evidence showing Vangl2 interaction
434 with other PCP proteins in auditory hair cells by utilizing the *Looptail* mutant. Inhibiting the
435 secretion of Wnt ligands, including Wnt5a, in a heterozygous *Looptail* background aggravates
436 defects in cochlear extension and sensory hair cell polarization (Najarro et al., 2020). Loss of
437 Fzd1 or Fzd2 causes mis-orientations of hair cells only when Vangl2 activity is also reduced (Yu
438 et al., 2010). Although *Ankrd6* mutant mice show disrupted uniform orientation of hair cells in the
439 utricle, only *Ankrd6* and *Vangl2* compound mutants display defective hair cell polarity and
440 patterning in the cochlea (Jones et al., 2014). Fat4 cooperates with Vangl2 to regulate cochlear
441 elongation and sensory epithelium patterning (Saburi et al., 2012). There are also physical and
442 genetic interactions between Scrib and Vangl2 in the planar polarization of stereociliary bundles
443 (Montcouquiol et al., 2003, 2006). It is possible that the *Looptail* mutation contributes partially to

444 enhance hair cell phenotypes because the resulting dysfunctional Vangl2 protein can interfere
445 with the proper localization of other PCP complexes.

446 During post-natal development, loss of Vangl2 has mild effects on the orientation of
447 auditory stereociliary bundles and on hearing loss, but mostly causes profound changes in the
448 shape and distribution of supporting cells that are necessary for cochlear amplification mediated
449 by OHCs (Copley et al., 2013). Thus, it will be of interest to determine the post-natal requirement
450 of other PCP proteins in maintaining hearing function.

451 Intriguingly, PCP proteins can function in parallel to instruct hair cell orientation. Zebrafish
452 lateral line neuromasts also consist of mechanosensory hair cells and support cells. Loss of
453 Vangl2 directly leads to PCP-dependent defects in hair cells. However, loss of Wnt11 or Fzd7
454 indirectly affects hair cell polarity by disrupting the alignment of support cells, suggesting a
455 contribution of support cells in sensory cell orientation (Navajas Acedo et al., 2019). Interestingly,
456 supporting cells can also dictate hair cell polarization in the mammalian cochlea. The
457 evolutionarily conserved transmembrane receptor protein tyrosine kinase 7 (PTK7) functions as a
458 vertebrate-specific PCP regulator. Disruption of PTK7 mostly affects stereociliary bundle
459 orientation in OHC3 (Lu et al., 2004). Mechanistically, PTK7 acts in parallel with Wnt/PCP
460 signaling to polarize hair cells by promoting junctional localization of myosin II near the apical
461 surfaces of supporting cells (Lee et al., 2012). Thus, PTK7 restricts the abnormal positioning of
462 kinocilia by exerting local tension at the neural edge of hair cells.

463 Cochlear OHCs are innervated by type II spiral ganglion neurons, which project peripheral
464 axons that extend beyond the IHCs and then turn 90° toward the cochlear base. Disruption of
465 Wnt secretion suggests that non-canonical Wnts are necessary to trigger Wnt/PCP signaling
466 during axon guidance (Ghimire and Deans, 2019). Fzd3 and Fzd6 are present at the basolateral
467 boundary between adjacent supporting cells along the trajectory of axonal growth cones; they
468 promote the asymmetric localization of Vangl2 and function redundantly to direct cochlear
469 innervation (Ghimire and Deans, 2019). Consequently, Vangl2 is enriched at intercellular
470 junctions between cochlear supporting cells and is non-autonomously required for axon turning
471 (Ghimire et al., 2018). Although it is unclear how Prickle1 and Prickle2 regulate hair cell polarity,

472 Prickle1 is required for neurite outgrowth of type II spiral ganglion neurons (Yang et al., 2017a).
473 Together, these observations demonstrate an essential role for Wnt/PCP signaling in hair cell
474 innervation.

475 Generally, dysfunctions of PCP proteins affect the uniform orientation of stereociliary
476 bundles between neighboring hair cells, but individual hair cells still retain polarized stereocilia
477 (Fig. 4B). This is because there are independent but nevertheless interconnected mechanisms
478 coordinating hair cell polarity. Intrinsic or intracellular PCP instructs hair bundle polarization within
479 a hair cell, while tissue-level or intercellular PCP establishes the uniform orientation of hair cells.
480 Indeed, several cytoskeletal regulatory proteins, such as Inscuteable (Insc), Partner of
481 Inscuteable (Pins), Cfp126 and Wdpcp, have been shown to control or restrict positioning of the
482 tubulin-based kinocilium and arrowhead-shaped distribution of actin-rich stereocilia (Ezan et al.,
483 2013; Tarchini et al., 2013; Cui et al., 2013; Gegg et al., 2014). Therefore, they can function to
484 establish intrinsic hair bundle polarity. However, the emergence of asymmetric hair bundle
485 position in the hair cell apical surface is tightly coupled with long-range orientation cues in the
486 tissue. Evidence is accumulating that G protein signaling functions to establish intrinsic
487 asymmetry and interpret intercellular PCP signaling. Accordingly, inhibition of Gai function leads
488 to randomized positioning of kinocilia and mis-orientations of OHCs (Tarchini et al., 2013). Daple,
489 a guanine nucleotide exchange factor and a Dvl-binding protein, mediates Wnt-stimulated
490 heterotrimeric G protein and phosphoinositide 3-kinase signaling to regulate both microtubule-
491 dependent eccentric kinocilium positioning and asymmetric localization of PCP proteins (Siletti et
492 al., 2017; Landin Malt et al., 2020). Therefore, a complex interplay between intracellular and
493 intercellular PCP signaling coordinates the acquisition of hair cell polarity.

494 **Proximal-distal limb outgrowth and elongation**

495 Vertebrate limb buds arise from the lateral plate mesoderm and its overlying ectoderm at
496 the presumptive forelimb and hindlimb locations. Dynamic formation of cellular protrusion and
497 biased orientation of cell division are major driving forces that elongate the limb bud along its
498 proximal-distal axis (Boehm et al., 2010; Wyngaarden et al., 2010). Wnt/PCP signaling plays an
499 essential role in regulating these directional cell behaviors (Barrow, 2011; Gao and Yang, 2013).

500 Early studies show that *Wnt5a* is expressed in the apical ectoderm ridge (AER) and distal
501 mesenchyme of the limb bud as a gradient along the proximal-distal axis (Gavin et al., 1990;
502 Dealy et al., 1993). Similarly, Vangl2 protein also displays a proximal-distal gradient of
503 asymmetric distribution (Gao et al., 2011).

504 *Wnt5a* plays an important role in establishing cell polarity for limb outgrowth (Fig. 4C).
505 Mice mutant for *Wnt5a* exhibit reduced individual skeletal elements, with absence of distal
506 phalanges (Yamaguchi et al., 1999). Analysis of cell behaviors by living imaging in mouse
507 embryos at E10.5 demonstrate that *Wnt5a* deficiency essentially disrupts the orientation of
508 mesenchymal cell movements and divisions toward the overlying ectoderm (Gros et al., 2010).
509 Conversely, implantation of *Wnt5a*-soaked beads into the lateral plate mesoderm of chick
510 embryos reveals that *Wnt5a* acts as a chemoattractant in the emerging limb bud to instruct
511 cellular polarization necessary for limb outgrowth (Wyngaarden et al., 2010). Moreover, locally
512 oriented cell shape changes and biased cell division planes are conserved cellular mechanisms
513 in vertebrate limb morphogenesis (Wyngaarden et al., 2010).

514 *Wnt5a* promotes the interaction between Ror2 and Vangl2 to establish the asymmetric
515 localization of Vangl2 in limb chondrocytes (Gao et al., 2011). It acts through Ror2 to induce a
516 proximal-distal gradient of Vangl2 phosphorylation in the mesenchyme, setting up a higher
517 Vangl2 activity in most distal cells (Gao et al., 2011). This phosphorylation is mediated by casein
518 kinase 1 and functions to polarize cellular behaviors of limb chondrocytes in a dose-dependent
519 manner (Yang et al., 2017b). *Wnt5a* and Vangl2 also show genetic interaction in limb skeletal
520 development. Reducing *Wnt5a* dosage in *Looptail* mice not only aggravates defects in distal limb
521 skeletal elements but also causes shortened long bones in the limb, reminiscent of Robinow
522 syndrome and brachydactyly type B (Wang et al., 2011). Therefore, a *Wnt5a* gradient provides
523 global cues, which are interpreted by Ror2 and Vangl2, to coordinate directional cellular
524 behaviors for proximal-distal limb elongation. Interestingly, *Wnt5a* can also generate mechanical
525 signals to trigger digit elongation likely through ROCK-mediated actomyosin contractility (Parada
526 et al., 2022). Loss of *Wnt5a* disrupts anisotropic active stresses and CE movements in
527 developing digits, leading to absence of digit-organizing centers (also known as phalange-forming

528 regions) and digit formation (Parada et al., 2022). Ror2 has been shown to regulate phalange
529 development mediated by the digit-organizing center (Witte et al., 2010). Thus, Wnt5a may
530 interact at least partially with Ror2 to combine mechanical cues and molecular signals in digit
531 emergence.

532 Other PCP proteins also contribute to limb outgrowth. Ryk regulates Wnt/PCP signaling
533 and limb elongation in part by promoting Vangl2 stability (Andre et al., 2012). Dvl family proteins
534 are required for Wnt5a-induced Vangl2 phosphorylation by facilitating the interaction of casein
535 kinase 1 and Vangl2 (Yang et al., 2017b). Mice deficient for Prickle1 show loss of one phalangeal
536 segment on digits 2-5 in both forelimbs and hindlimbs (Yang et al., 2013; Liu et al., 2014). Thus,
537 biochemical and functional interactions between PCP proteins are essential for proper limb
538 morphogenesis.

539 **Concluding remarks**

540 PCP proteins contribute to the highly choreographed cellular organization in many
541 morphogenetic processes. Extensive research has greatly advanced our understanding on their
542 implications in controlling asymmetric organogenesis and tissue homeostasis. Accumulating
543 evidence also suggest that dysfunctions of PCP proteins are linked to a variety of human
544 diseases. Nevertheless, there are still many intriguing questions that deserve further
545 investigation.

546 Although Wnt ligands can provide global cues to initiate cell polarity in several PCP-
547 dependent processes, it remains to be determined whether molecular pathways act in concert
548 with other orientation cues to instruct and establish PCP features. Interestingly, a recent research
549 shows that the orientation of tissue stretch cooperates with Wnt signaling gradient to align PCP in
550 *Xenopus* neuroectoderm (Hirano et al., 2022). Since mechanical constraints act as important
551 cues in planar polarization, it will be important to further develop interdisciplinary approaches for
552 understanding the interplay of PCP signaling and mechanotransduction in morphogenesis.
553 Functional gene disruptions combined with in vivo live imaging and manipulation of mechanical
554 state should help to push the field forward.

555 Another important aspect is to understand how cell polarity can be translated to cell fate
556 specification. These two processes are clearly interconnected in several contexts, such that
557 molecular asymmetry provided by PCP proteins helps to promote cell type-specific differentiation.
558 For example, cell polarity cues are coupled with cell lineage segregation during intestinal stem
559 cell self-renewal and differentiation (Böttcher et al., 2021). Deciphering the interaction between
560 molecular signals and mechanical forces in the coupling of cell fate decision and morphogenetic
561 movements also represents a significant challenge. In this regard, it is noteworthy that Wnt5a
562 signaling functions in a mechanical feedback that links specification and elongation of developing
563 digits (Parada et al., 2022).

564 The formation of separately localized “core” PCP protein complexes is important to create
565 cellular polarization. What are the exact roles of each complex in the coordination of polarized
566 cellular behaviors? How do they converge to regulate cell polarity? Similarly, it is unclear how and
567 when the “core” PCP pathway and the Fat/Dchs polarity module coordinate to regulate polarized
568 cellular behaviors. In *Drosophila*, it appears that they may be coupled by specific Prickle isoforms
569 through regulation of microtubule plus-end bias (Strutt and Strutt, 2021). Whether this is
570 conserved in vertebrates awaits future investigation. Therefore, future research using both
571 invertebrate and vertebrate PCP systems will certainly bring important breakthrough for some of
572 these issues and provide the link between PCP protein dysfunctions and human diseases.

573

573 **Conflict of interest**

574 The authors declare no competing interests.

575 **Acknowledgments**

576 I would like to apologize for being unable to include many studies in the discussion due to space
577 limitations. This work was supported by grants from the National Natural Science Foundation of
578 China (grant number 32070813), the French Muscular Dystrophy Association (AFM-Téléthon
579 grant number 23545), the Centre National de la Recherche Scientifique (CNRS), and the
580 Sorbonne University.

581

- 581 **References**
- 582 Adler, P.N., Wallingford, J.B., 2017. From planar cell polarity to ciliogenesis and back: The curious tale of
- 583 the PPE and CPLANE proteins. *Trends Cell Biol.* 27, 379–390.
- 584 Ajima, R., Bisson, J.A., Helt, J.C., Nakaya, M.A., Habas, R., Tessarollo, L., He, X., Morrissey, E.E.,
- 585 Yamaguchi, T.P., Cohen, E.D., 2015. DAAM1 and DAAM2 are co-required for myocardial maturation
- 586 and sarcomere assembly. *Dev. Biol.* 408, 126–139.
- 587 Andre, P., Wang, Q., Wang, N., Gao, B., Schilit, A., Halford, M.M., Stacker, S.A., Zhang, X., Yang, Y.,
- 588 2012. The Wnt coreceptor Ryk regulates Wnt/planar cell polarity by modulating the degradation of the
- 589 core planar cell polarity component Vangl2. *J. Biol. Chem.* 287, 44518–44525.
- 590 Antic, D., Stubbs, J.L., Suyama, K., Kintner, C., Scott, M.P., Axelrod, J.D., 2010. Planar cell polarity
- 591 enables posterior localization of nodal cilia and left-right axis determination during mouse and *Xenopus*
- 592 embryogenesis. *PLoS One* 5, e8999.
- 593 Axelrod, J.D., 2020. Planar cell polarity signaling in the development of left-right asymmetry. *Curr. Opin.*
- 594 *Cell Biol.* 62, 61–69.
- 595 Bagherie-Lachidan, M., Reginensi, A., Pan, Q., Zaveri, H.P., Scott, D.A., Blencowe, B.J., Helmbacher, F.,
- 596 McNeill, H., 2015. Stromal Fat4 acts non-autonomously with Dchs1/2 to restrict the nephron progenitor
- 597 pool. *Development* 142, 2564–2573.
- 598 Barrow, J., 2011. Wnt/planar cell polarity signaling: an important mechanism to coordinate growth and
- 599 patterning in the limb. *Organogenesis* 7, 260–266.
- 600 Bellchambers, H.M., Ware, S.M., 2021. Loss of *Zic3* impairs planar cell polarity leading to abnormal left-
- 601 right signaling, heart defects and neural tube defects. *Hum. Mol. Genet.* 30, 2402–2415.
- 602 Blair, S., McNeill, H., 2018. Big roles for Fat cadherins. *Curr. Opin. Cell Biol.* 51, 73–80.
- 603 Boehm, B., Westerberg, H., Lesnicar-Pucko, G., Raja, S., Rautschka, M., Cotterell, J., Swoger, J., Sharpe,
- 604 J., 2010. The role of spatially controlled cell proliferation in limb bud morphogenesis. *PLoS Biol.* 8,
- 605 e1000420.
- 606 Borovina, A., Superina, S., Voskas, D., Ciruna, B., 2010. Vangl2 directs the posterior tilting and asymmetric
- 607 localization of motile primary cilia. *Nat. Cell Biol.* 12, 407–412.
- 608 Böttcher, A., Büttner, M., Tritschler, S., Sterr, M., Aliluev, A., Oppenländer, L., Burtscher, I., Sass, S.,
- 609 Irmiler, M., Beckers, J., et al., 2021. Non-canonical Wnt/PCP signalling regulates intestinal stem cell
- 610 lineage priming towards enteroendocrine and Paneth cell fates. *Nat. Cell Biol.* 23, 23–31.
- 611 Brzóska, H.Ł., d'Esposito, A.M., Kolatsi-Joannou, M., Patel, V., Igarashi, P., Lei, Y., Finnell, R.H., Lythgoe,
- 612 M.F., Woolf, A.S., Papakrivopoulou, E., et al., 2016. Planar cell polarity genes *Celsr1* and *Vangl2* are
- 613 necessary for kidney growth, differentiation, and rostrocaudal patterning. *Kidney Int.* 90, 1274–1284.
- 614 Carroll, T.J., Yu, J., 2012. The kidney and planar cell polarity. *Curr. Top. Dev. Biol.* 101, 185–212.
- 615 Cervantes, S., Yamaguchi, T.P., Hebrok, M., 2009. *Wnt5a* is essential for intestinal elongation in mice.
- 616 *Dev. Biol.* 326, 285–294.
- 617 Cheong, S.S., Akram, K.M., Matellan, C., Kim, S.Y., Gaboriau, D.C.A., Hind, M., Del Río Hernández, A.E.,
- 618 Griffiths, M., Dean, C.H., 2020. The planar polarity component VANGL2 is a key regulator of
- 619 mechanosignaling. *Front. Cell Dev. Biol.* 8, 577201.
- 620 Chu, C.W., Ossipova, O., Ioannou, A., Sokol, S.Y., 2016. Prickle3 synergizes with *Wtip* to regulate basal
- 621 body organization and cilia growth. *Sci. Rep.* 6, 24104.
- 622 Copley, C.O., Duncan, J.S., Liu, C., Cheng, H., Deans, M.R., 2013. Postnatal refinement of auditory hair
- 623 cell planar polarity deficits occurs in the absence of *Vangl2*. *J. Neurosci.* 33, 14001–14016.
- 624 Cui, C., Chatterjee, B., Lozito, T.P., Zhang, Z., Francis, R.J., Yagi, H., Swanhart, L.M., Sanker, S., Francis,
- 625 D., Yu, Q., et al., 2013. *Wdpcp*, a PCP protein required for ciliogenesis, regulates directional cell
- 626 migration and cell polarity by direct modulation of the actin cytoskeleton. *PLoS Biol.* 11, e1001720.
- 627 Curtin, J.A., Quint, E., Tsipouri, V., Arkell, R.M., Cattanch, B., Copp, A.J., Henderson, D.J., Spurr, N.,
- 628 Stanier, P., Fisher, E.M., et al., 2003. Mutation of *Celsr1* disrupts planar polarity of inner ear hair cells
- 629 and causes severe neural tube defects in the mouse. *Curr. Biol.* 13, 1129–1133.
- 630 Das, A., Tanigawa, S., Karner, C.M., Xin, M., Lum, L., Chen, C., Olson, E.N., Perantoni, A.O., Carroll, T.J.,
- 631 2013. Stromal-epithelial crosstalk regulates kidney progenitor cell differentiation. *Nat. Cell Biol.* 15,
- 632 1035–1044.
- 633 Dealy, C.N., Roth, A., Ferrari, D., Brown, A.M., Kosher, R.A., 1993. *Wnt-5a* and *Wnt-7a* are expressed in
- 634 the developing chick limb bud in a manner suggesting roles in pattern formation along the proximodistal
- 635 and dorsoventral axes. *Mech. Dev.* 43, 175–186.
- 636 Deans, M.R., Antic, D., Suyama, K., Scott, M.P., Axelrod, J.D., Goodrich, L.V., 2007. Asymmetric
- 637 distribution of prickle-like 2 reveals an early underlying polarization of vestibular sensory epithelia in the
- 638 inner ear. *J. Neurosci.* 27, 3139–3147.

639 Derish, I., Lee, J.K.H., Wong-King-Cheong, M., Babayeva, S., Caplan, J., Leung, V., Shahinian, C., Gravel,
640 M., Deans, M.R., Gros, P., et al., 2020. Differential role of planar cell polarity gene *Vangl2* in embryonic
641 and adult mammalian kidneys. *PLoS One* 15, e0230586.

642 Derrick, C.J., Santos-Ledo, A., Eley, L., Henderson, D.J., Chaudhry, B., 2022. Sequential action of *jnk*
643 genes establishes the embryonic left-right axis. *Development* 149, dev200136.

644 Descamps, B., Sewduth, R., Ferreira Tojais, N., Jaspard, B., Reynaud, A., Sohet, F., Lacolley, P., Allières,
645 C., Lamazière, J.M., Moreau, C., et al., 2012. Frizzled 4 regulates arterial network organization through
646 noncanonical Wnt/planar cell polarity signaling. *Circ. Res.* 110, 47–58.

647 Desgrange, A., Le Garrec, J.F., Meilhac, S.M., 2018. Left-right asymmetry in heart development and
648 disease: forming the right loop. *Development* 145, dev162776.

649 Driver, E.C., Northrop, A., Kelley, M.W., 2017. Cell migration, intercalation and growth regulate mammalian
650 cochlear extension. *Development* 144, 3766–3776.

651 Duncan, J.S., Stoller, M.L., Francl, A.F., Tissir, F., Devenport, D., Deans, M.R., 2017. *Celsr1* coordinates
652 the planar polarity of vestibular hair cells during inner ear development. *Dev. Biol.* 423, 126–137.

653 Dush, M.K., Nascone-Yoder, N.M., 2019. *Vangl2* coordinates cell rearrangements during gut elongation.
654 *Dev. Dyn.* 248, 569–582.

655 Ezan, J., Lasvaux, L., Gezer, A., Novakovic, A., May-Simera, H., Belotti, E., Lhoumeau, A.C., Birnbaumer,
656 L., Beer-Hammer, S., Borg, J.P., et al., 2013. Primary cilium migration depends on G-protein signalling
657 control of subapical cytoskeleton. *Nat. Cell Biol.* 15, 1107–1115.

658 Gao, B., Song, H., Bishop, K., Elliot, G., Garrett, L., English, M.A., Andre, P., Robinson, J., Sood, R.,
659 Minami, Y., et al., 2011. Wnt signaling gradients establish planar cell polarity by inducing *Vangl2*
660 phosphorylation through *Ror2*. *Dev. Cell* 20, 163–176.

661 Gao, B., Yang, Y., 2013. Planar cell polarity in vertebrate limb morphogenesis. *Curr. Opin. Genet. Dev.* 23,
662 438–444.

663 Gavin, B.J., McMahon, J.A., McMahon, A.P., 1990. Expression of multiple novel Wnt-1/int-1-related genes
664 during fetal and adult mouse development. *Genes Dev.* 4, 2319–2332.

665 Gegg, M., Böttcher, A., Burtscher, I., Hasenoeder, S., Van Campenhout, C., Aichler, M., Walch, A., Grant,
666 S.G., Lickert, H., 2014. Flattop regulates basal body docking and positioning in mono- and multiciliated
667 cells. *Elife* 3, e03842.

668 Ghimire, S.R., Deans, M.R., 2019. Frizzled3 and frizzled6 cooperate with *Vangl2* to direct cochlear
669 innervation by type II spiral ganglion neurons. *J. Neurosci.* 39, 8013–8023.

670 Ghimire, S.R., Ratzan, E.M., Deans, M.R., 2018. A non-autonomous function of the core PCP protein
671 *VANGL2* directs peripheral axon turning in the developing cochlea. *Development* 145, dev159012.

672 Gibbs, B.C., Damerla, R.R., Vldar, E.K., Chatterjee, B., Wan, Y., Liu, X., Cui, C., Gabriel, G.C., Zahid, M.,
673 Yagi, H., et al., 2016. *Prickle1* mutation causes planar cell polarity and directional cell migration defects
674 associated with cardiac outflow tract anomalies and other structural birth defects. *Biol. Open* 5, 323–
675 335.

676 Giese, A.P., Ezan, J., Wang, L., Lasvaux, L., Lembo, F., Mazzocco, C., Richard, E., Reboul, J., Borg, J.P.,
677 Kelley, M.W., et al., 2012. *Gipc1* has a dual role in *Vangl2* trafficking and hair bundle integrity in the
678 inner ear. *Development* 139, 3775–3785.

679 Grimes, D.T., Burdine, R.D., 2017. Left-right patterning: Breaking symmetry to asymmetric morphogenesis.
680 *Trends Genet.* 33, 616–628.

681 Gros, J., Hu, J.K., Vinegoni, C., Feruglio, P.F., Weissleder, R., Tabin, C.J., 2010. WNT5A/JNK and
682 FGF/MAPK pathways regulate the cellular events shaping the vertebrate limb bud. *Curr. Biol.* 1993–
683 2002.

684 Grzymkowski, J., Wyatt, B., Nascone-Yoder, N., 2020. The twists and turns of left-right asymmetric gut
685 morphogenesis. *Development* 147, dev187583.

686 Gubb, D., García-Bellido, A., 1982. A genetic analysis of the determination of cuticular polarity during
687 development in *Drosophila melanogaster*. *J. Embryol. Exp. Morphol.* 68, 37–57.

688 Hashimoto, M., Shinohara, K., Wang, J., Ikeuchi, S., Yoshida, S., Meno, C., Nonaka, S., Takada, S., Hatta,
689 K., Wynshaw-Boris, A., et al., 2010. Planar polarization of node cells determines the rotational axis of
690 node cilia. *Nat. Cell Biol.* 12, 170–176.

691 Henderson, D.J., Long, D.A., Dean, C.H., 2018. Planar cell polarity in organ formation. *Curr. Opin. Cell*
692 *Biol.* 55, 96–103.

693 Henderson, D.J., Phillips, H.M., Chaudhry, B., 2006. Vang-like 2 and noncanonical Wnt signaling in outflow
694 tract development. *Trends Cardiovasc. Med.* 16, 38–45.

695 Hirano, S., Mii, Y., Charras, G., Michiue, T., 2022. Alignment of cell long axis by unidirectional tension acts
696 cooperatively with Wnt signalling to establish PCP. *Development* 149, dev.200515.

697 Huycke, T.R., Tabin, C.J., 2018. Chick midgut morphogenesis. *Int. J. Dev. Biol.* 62, 109–119.

698 Jones, C., Qian, D., Kim, S.M., Li, S., Ren, D., Knapp, L., Sprinzak, D., Avraham, K.B., Matsuzaki, F., Chi,
699 F., et al., 2014. Ankrd6 is a mammalian functional homolog of *Drosophila* planar cell polarity gene *diego*
700 and regulates coordinated cellular orientation in the mouse inner ear. *Dev. Biol.* 395, 62–72.

701 Juan, T., Géminard, C., Coutelis, J.B., Cerezo, D., Polès, S., Noselli, S., Fürthauer, M., 2018. Myosin1D is
702 an evolutionarily conserved regulator of animal left-right asymmetry. *Nat. Commun.* 9, 1942.

703 Kadzik, R.S., Cohen, E.D., Morley, M.P., Stewart, K.M., Lu, M.M., Morrisey, E.E., 2014. Wnt ligand/Frizzled
704 2 receptor signaling regulates tube shape and branch-point formation in the lung through control of
705 epithelial cell shape. *Proc. Natl. Acad. Sci. U. S. A.* 111, 12444–12449x.

706 Karner, C.M., Chirumamilla, R., Aoki, S., Igarashi, P., Wallingford, J.B., Carroll, T.J., 2009. Wnt9b signaling
707 regulates planar cell polarity and kidney tubule morphogenesis. *Nat. Genet.* 41, 793–799.

708 Kishimoto, K., Tamura, M., Nishita, M., Minami, Y., Yamaoka, A., Abe, T., Shigeta, M., Morimoto, M., 2018.
709 Synchronized mesenchymal cell polarization and differentiation shape the formation of the murine
710 trachea and esophagus. *Nat. Commun.* 9, 2816.

711 Kispert, A., Vainio, S., McMahon, A.P., 1998. Wnt-4 is a mesenchymal signal for epithelial transformation of
712 metanephric mesenchyme in the developing kidney. *Development* 125, 4225–4234.

713 Krneta-Stankic, V., Corkins, M.E., Paulucci-Holthausen, A., Kloc, M., Gladden, A.B., Miller, R.K., 2021. The
714 Wnt/PCP formin Daam1 drives cell-cell adhesion during nephron development. *Cell Rep.* 36, 109340.

715 Kunimoto, K., Bayly, R.D., Vladar, E.K., Vonderfecht, T., Gallagher, A.R., Axelrod, J.D., 2017. Disruption of
716 core planar cell polarity signaling regulates renal tubule morphogenesis but is not cystogenic. *Curr. Biol.*
717 27, 3120–3131.e4.

718 Landin Malt, A., Hogan, A.K., Smith, C.D., Madani, M.S., Lu, X., 2020. Wnts regulate planar cell polarity via
719 heterotrimeric G protein and PI3K signaling. *J. Cell Biol.* 219, e201912071.

720 Lavalou, J., Lecuit, T., 2022. In search of conserved principles of planar cell polarization. *Curr. Opin.*
721 *Genet. Dev.* 72, 69–81.

722 Lawrence, P.A., Shelton, P.M., 1975. The determination of polarity in the developing insect retina. *J.*
723 *Embryol. Exp. Morphol.* 33, 471–486.

724 Lee, H.J., Shi, D.L., Zheng, J.J., 2015. Conformational change of Dishevelled plays a key regulatory role in
725 the Wnt signaling pathways. *Elife* 4, e08142.

726 Lee, J., Andreeva, A., Sipe, C.W., Liu, L., Cheng, A., Lu, X., 2012. PTK7 regulates myosin II activity to
727 orient planar polarity in the mammalian auditory epithelium. *Curr. Biol.* 22, 956–966.

728 Li, C., Smith, S.M., Peinado, N., Gao, F., Li, W., Lee, M.K., Zhou, B., Bellusci, S., Pryhuber, G.S., Ho, H.H.,
729 et al., 2020. WNT5a-ROR signaling is essential for alveologenesis. *Cells* 9, 384.

730 Li, D., Angermeier, A., Wang, J., 2019. Planar cell polarity signaling regulates polarized second heart field
731 morphogenesis to promote both arterial and venous pole septation. *Development* 146, dev181719.

732 Li, D., Hallett, M.A., Zhu, W., Rubart, M., Liu, Y., Yang, Z., Chen, H., Haneline, L.S., Chan, R.J., Schwartz,
733 R.J., et al., 2011. Dishevelled-associated activator of morphogenesis 1 (Daam1) is required for heart
734 morphogenesis. *Development* 138, 303–315.

735 Lienkamp, S.S., Liu, K., Karner, C.M., Carroll, T.J., Ronneberger, O., Wallingford, J.B., Walz, G., 2012.
736 Vertebrate kidney tubules elongate using a planar cell polarity-dependent, rosette-based mechanism of
737 convergent extension. *Nat. Genet.* 44, 1382–1387.

738 Little, R.B., Norris, D.P., 2021. Right, left and cilia: How asymmetry is established. *Semin. Cell Dev. Biol.*
739 110, 11–18.

740 Liu, C., Lin, C., Gao, C., May-Simera, H., Swaroop, A., Li, T., 2014. Null and hypomorph Prickle1 alleles in
741 mice phenocopy human Robinow syndrome and disrupt signaling downstream of Wnt5a. *Biol. Open* 3,
742 861–870.

743 Loscertales, M., Mikels, A.J., Hu, J.K., Donahoe, P.K., Roberts, D.J., 2008. Chick pulmonary Wnt5a directs
744 airway and vascular tubulogenesis. *Development* 135, 1365–1376.

745 Lu, X., Borchers, A.G., Jolicoeur, C., Rayburn, H., Baker, J.C., Tessier-Lavigne, M., 2004. PTK7/CCK-4 is
746 a novel regulator of planar cell polarity in vertebrates. *Nature* 430, 93–98.

747 Mao, Y., Francis-West, P., Irvine, K.D., 2015. Fat4/Dchs1 signaling between stromal and cap mesenchyme
748 cells influences nephrogenesis and ureteric bud branching. *Development* 142, 2574–2585.

749 Matsuyama, M., Aizawa, S., Shimono, A., 2009. Sfrp controls apicobasal polarity and oriented cell division
750 in developing gut epithelium. *PLoS Genet.* 5, e1000427.

751 May-Simera, H., Kelley, M.W., 2012. Planar cell polarity in the inner ear. *Curr. Top. Dev. Biol.* 101, 111–
752 140.

753 Merks, A.M., Swinarski, M., Meyer, A.M., Müller, N.V., Özcan, I., Donat, S., Burger, A., Gilbert, S.,
754 Mosimann, C., Abdelilah-Seyfried, S., et al., 2018. Planar cell polarity signalling coordinates heart tube
755 remodelling through tissue-scale polarisation of actomyosin activity. *Nat. Commun.* 9, 2161.

756 Milgrom-Hoffman, M., Humbert, P.O., 2018. Regulation of cellular and PCP signalling by the Scribble
757 polarity module. *Semin. Cell Dev. Biol.* 81, 33–45.

758 Miller, R.K., Canny, S.G., Jang, C.W., Cho, K., Ji, H., Wagner, D.S., Jones, E.A., Habas, R., McCrea, P.D.,
759 2011. Pronephric tubulogenesis requires Daam1-mediated planar cell polarity signaling. *J. Am. Soc.*
760 *Nephrol.* 22, 1654–1664.

761 Minegishi, K., Hashimoto, M., Ajima, R., Takaoka, K., Shinohara, K., Ikawa, Y., Nishimura, H., McMahon,
762 A.P., Willert, K., Okada, Y., et al., 2017. A Wnt5 activity asymmetry and intercellular signaling via PCP
763 proteins polarize node cells for left-right symmetry breaking. *Dev. Cell* 40, 439–452.e4.

764 Montcouquiol, M., Rachel, R.A., Lanford, P.J., Copeland, N.G., Jenkins, N.A., Kelley, M.W., 2003.
765 Identification of *Vangl2* and *Scrb1* as planar polarity genes in mammals. *Nature* 423, 173–177.

766 Montcouquiol, M., Sans, N., Huss, D., Kach, J., Dickman, J.D., Forge, A., Rachel, R.A., Copeland, N.G.,
767 Jenkins, N.A., Bogani, D., et al., 2006. Asymmetric localization of *Vangl2* and *Fz3* indicate novel
768 mechanisms for planar cell polarity in mammals. *J. Neurosci.* 26, 5265–5275.

769 Najarro, E.H., Huang, J., Jacobo, A., Quiruz, L.A., Grillet, N., Cheng, A.G., 2020. Dual regulation of planar
770 polarization by secreted Wnts and *Vangl2* in the developing mouse cochlea. *Development* 147,
771 dev191981.

772 Navajas Acedo, J., Voas, M.G., Alexander, R., Woolley, T., Unruh, J.R., Li, H., Moens, C., Piotrowski, T.,
773 2019. PCP and Wnt pathway components act in parallel during zebrafish mechanosensory hair cell
774 orientation. *Nat. Commun.* 10, 3993.

775 Nishita, M., Qiao, S., Miyamoto, M., Okinaka, Y., Yamada, M., Hashimoto, R., Iijima, K., Otani, H.,
776 Hartmann, C., Nishinakamura, R., et al., 2014. Role of *Wnt5a-Ror2* signaling in morphogenesis of the
777 metanephric mesenchyme during ureteric budding. *Mol. Cell. Biol.* 34, 3096–3105.

778 O'Brien, L.L., Combes, A.N., Short, K.M., Lindström, N.O., Whitney, P.H., Cullen-McEwen, L.A., Ju, A.,
779 Abdelhalim, A., Michos, O., Bertram, J.F., et al., 2018. *Wnt11* directs nephron progenitor polarity and
780 motile behavior ultimately determining nephron endowment. *Elife* 7, e40392.

781 Parada, C., Banavar, S.P., Khalilian, P., Rigaud, S., Michaut, A., Liu, Y., Joshy, D.M., Campàs, O., Gros,
782 J., 2022. Mechanical feedback defines organizing centers to drive digit emergence. *Dev. Cell* 57, 854–
783 866.e6.

784 Phillips, H.M., Hildreth, V., Peat, J.D., Murdoch, J.N., Kobayashi, K., Chaudhry, B., Henderson, D.J., 2008.
785 Non-cell-autonomous roles for the planar cell polarity gene *Vangl2* in development of the coronary
786 circulation. *Circ. Res.* 102, 615–623.

787 Phillips, H.M., Murdoch, J.N., Chaudhry, B., Copp, A.J., Henderson, D.J., 2005. *Vangl2* acts via RhoA
788 signaling to regulate polarized cell movements during development of the proximal outflow tract. *Circ.*
789 *Res.* 96, 292–299.

790 Poobalasingam, T., Yates, L.L., Walker, S.A., Pereira, M., Gross, N.Y., Ali, A., Kolatsi-Joannou, M.,
791 Jarvelin, M.R., Pekkanen, J., Papakrivopoulou, E., et al., 2017. Heterozygous *Vangl2*(Looptail) mice
792 reveal novel roles for the planar cell polarity pathway in adult lung homeostasis and repair. *Dis. Model*
793 *Mech.* 10, 409–423.

794 Ramsbottom, S.A., Sharma, V., Rhee, H.J., Eley, L., Phillips, H.M., Rigby, H.F., Dean, C., Chaudhry, B.,
795 Henderson, D.J., 2014. *Vangl2*-regulated polarisation of second heart field-derived cells is required for
796 outflow tract lengthening during cardiac development. *PLoS Genet.* 10, e1004871.

797 Rao-Bhatia, A., Zhu, M., Yin, W.C., Coquenlorge, S., Zhang, X., Woo, J., Sun, Y., Dean, C.H., Liu, A., Hui,
798 C.C., et al., 2020. Hedgehog-activated *Fat4* and PCP pathways mediate mesenchymal cell clustering
799 and villus formation in gut development. *Dev. Cell* 52, 647–658.e6.

800 Rocque, B.L., Babayeva, S., Li, J., Leung, V., Nezvitsky, L., Cybulsky, A.V., Gros, P., Torban, E., 2015.
801 Deficiency of the planar cell polarity protein *Vangl2* in podocytes affects glomerular morphogenesis and
802 increases susceptibility to injury. *J. Am. Soc. Nephrol.* 26, 576–586.

803 Saburi, S., Hester, I., Fischer, E., Pontoglio, M., Eremina, V., Gessler, M., Quaggin, S.E., Harrison, R.,
804 Mount, R., McNeill, H., 2008. Loss of *Fat4* disrupts PCP signaling and oriented cell division and leads to
805 cystic kidney disease. *Nat. Genet.* 40, 1010–1015.

806 Saburi, S., Hester, I., Goodrich, L., McNeill, H., 2012. Functional interactions between *Fat* family cadherins
807 in tissue morphogenesis and planar polarity. *Development* 139, 1806–1820.

808 Sai, X., Ikawa, Y., Nishimura, H., Mizuno, K., Kajikawa, E., Katoh, T.A., Kimura, T., Shiratori, H., Takaoka,
809 K., Hamada, H., et al., 2022. Planar cell polarity-dependent asymmetric organization of microtubules for
810 polarized positioning of the basal body in node cells. *Development* 149, dev200315.

811 Savin, T., Kurpios, N.A., Shyer, A.E., Florescu, P., Liang, H., Mahadevan, L., Tabin, C.J., 2011. On the
812 growth and form of the gut. *Nature* 476, 57–62.

813 Shi, D.L., 2020. Decoding Dishevelled-mediated Wnt signaling in vertebrate early development. *Front. Cell*
814 *Dev. Biol.* 8, 588370.

815 Shoshkes-Carmel, M., Wang, Y.J., Wangenstein, K.J., Tóth, B., Kondo, A., Massasa, E.E., Itzkovitz, S.,
816 Kaestner, K.H., 2018. Subepithelial telocytes are an important source of Wnts that supports intestinal
817 crypts. *Nature* 557, 242–246.

818 Siletti, K., Tarchini, B., Hudspeth, A.J., 2017. Daple coordinates organ-wide and cell-intrinsic polarity to
819 pattern inner-ear hair bundles. *Proc. Natl. Acad. Sci. U. S. A.* 114, E11170–E11179.

820 Sinha, T., Li, D., Théveniau-Ruissy, M., Hutson, M.R., Kelly, R.G., Wang, J., 2015. Loss of *Wnt5a* disrupts
821 second heart field cell deployment and may contribute to OFT malformations in DiGeorge syndrome.
822 *Hum. Mol. Genet.* 24, 1704–1716.

823 Sinha, T., Wang, B., Evans, S., Wynshaw-Boris, A., Wang, J., 2012. Disheveled mediated planar cell
824 polarity signaling is required in the second heart field lineage for outflow tract morphogenesis. *Dev. Biol.*
825 370, 135–144.

826 Skouloudaki, K., Puetz, M., Simons, M., Courbard, J.R., Boehlke, C., Hartleben, B., Engel, C., Moeller,
827 M.J., Englert, C., Bollig, F., et al., 2009. Scribble participates in Hippo signaling and is required for
828 normal zebrafish pronephros development. *Proc. Natl. Acad. Sci. U. S. A.* 106, 8579–8584.

829 Song, H., Hu, J., Chen, W., Elliott, G., Andre, P., Gao, B., Yang, Y., 2010. Planar cell polarity breaks
830 bilateral symmetry by controlling ciliary positioning. *Nature* 466, 378–382.

831 Stark, K., Vainio, S., Vassileva, G., McMahon, A.P., 1994. Epithelial transformation of metanephric
832 mesenchyme in the developing kidney regulated by *Wnt-4*. *Nature* 372, 679–683.

833 Strutt, H., Strutt, D., 2021. How do the Fat-Dachsous and core planar polarity pathways act together and
834 independently to coordinate polarized cell behaviours? *Open Biol.* 11, 200356.

835 Tarchini, B., Jolicoeur, C., Cayouette, M., 2013. A molecular blueprint at the apical surface establishes
836 planar asymmetry in cochlear hair cells. *Dev. Cell* 27, 88–102.

837 Tingler, M., Kurz, S., Maerker, M., Ott, T., Fuhl, F., Schweickert, A., LeBlanc-Straceski, J.M., Noselli, S.,
838 Blum, M., 2018. A conserved role of the unconventional Myosin 1d in laterality determination. *Curr. Biol.*
839 28, 810–816.e3.

840 Torban, E., Sokol, S.Y., 2021. Planar cell polarity pathway in kidney development, function and disease.
841 *Nat. Rev. Nephrol.* 17, 369–385.

842 Vladar, E.K., Bayly, R.D., Sangoram, A.M., Scott, M.P., Axelrod, J.D., 2012. Microtubules enable the planar
843 cell polarity of airway cilia. *Curr. Biol.* 22, 2203–2212.

844 Vladar, E.K., Königshoff, M., 2020. Noncanonical Wnt planar cell polarity signaling in lung development
845 and disease. *Biochem. Soc. Trans.* 48, 231–243.

846 Vladar, E.K., Nayak, J.V., Milla, C.E., Axelrod, J.D., 2016. Airway epithelial homeostasis and planar cell
847 polarity signaling depend on multiciliated cell differentiation. *JCI Insight* 1, e88027.

848 Wallingford, J.B., 2012. Planar cell polarity and the developmental control of cell behavior in vertebrate
849 embryos. *Annu. Rev. Cell Dev. Biol.* 28, 627–653.

850 Wang, B., Sinha, T., Jiao, K., Serra, R., Wang, J., 2011. Disruption of PCP signaling causes limb
851 morphogenesis and skeletal defects and may underlie Robinow syndrome and brachydactyly type B.
852 *Hum. Mol. Genet.* 20, 271–285.

853 Wang, I.Y., Chung, C.F., Babayeva, S., Sogomonian, T., Torban E., 2021. Loss of planar cell polarity
854 effector Fuzzy causes renal hypoplasia by disrupting several signaling pathways. *J. Dev. Biol.* 10, 1.

855 Wang, J., Mark, S., Zhang, X., Qian, D., Yoo, S.J., Radde-Gallwitz, K., Zhang, Y., Lin, X., Collazo, A.,
856 Wynshaw-Boris, A., et al., 2005. Regulation of polarized extension and planar cell polarity in the cochlea
857 by the vertebrate PCP pathway. *Nat. Genet.* 37, 980–985.

858 Wang, M., Marco, P., Capra, V., Kibar, Z., 2019. Update on the role of the non-canonical Wnt/planar cell
859 polarity pathway in neural tube defects. *Cells* 8, 1198.

860 Wang, S., Cebrian, C., Schnell, S., Gumucio, D.L., 2018. Radial WNT5A-guided post-mitotic filopodial
861 pathfinding is critical for midgut tube elongation. *Dev. Cell* 46, 173–188.e3.

862 Wang, S., Roy, J.P., Tomlinson, A.J., Wang, E.B., Tsai, Y.H., Cameron, L., Underwood, J., Spence, J.R.,
863 Walton, K.D., Stacker, S.A., et al., 2020. RYK-mediated filopodial pathfinding facilitates midgut
864 elongation. *Development* 147, dev195388.

865 Wang, Y., Guo, N., Nathans, J., 2006. The role of *Frizzled3* and *Frizzled6* in neural tube closure and in the
866 planar polarity of inner ear sensory hair cells. *J. Neurosci.* 26, 2147–2156.

867 Welsh, I.C., Thomsen, M., Gludish, D.W., Alfonso-Parra, C., Bai, Y., Martin, J.F., Kurpios, N.A., 2013.
868 Integration of left-right *Pitx2* transcription and Wnt signaling drives asymmetric gut morphogenesis via
869 *Daam2*. *Dev. Cell* 26, 629–644.

870 Witte, F., Chan, D., Economides, A.N., Mundlos, S., Stricker, S., 2010. Receptor tyrosine kinase-like
871 orphan receptor 2 (ROR2) and Indian hedgehog regulate digit outgrowth mediated by the phalanx-
872 forming region. *Proc. Natl. Acad. Sci. U. S. A.* 107, 14211–14216.

873 Wyngaarden, L.A., Vogelii, K.M., Ciruna, B.G., Wells, M., Hadjantonakis, A.K., Hopyan, S., 2010. Oriented
874 cell motility and division underlie early limb bud morphogenesis. *Development* 137, 2551–2558.

875 Yamaguchi, T.P., Bradley, A., McMahon, A.P., Jones, S., 1999. A *Wnt5a* pathway underlies outgrowth of
876 multiple structures in the vertebrate embryo. *Development* 126, 1211–1223.

877 Yang, T., Bassuk, A.G., Fritsch, B., 2013. Prickle1 stunts limb growth through alteration of cell polarity and
878 gene expression. *Dev. Dyn.* 242, 1293–1306.

879 Yang, T., Kersigo, J., Wu, S., Fritsch, B., Bassuk, A.G., 2017a. Prickle1 regulates neurite outgrowth of
880 apical spiral ganglion neurons but not hair cell polarity in the murine cochlea. *PLoS One* 12, e0183773.

881 Yang, W., Garrett, L., Feng, D., Elliott, G., Liu, X., Wang, N., Wong, Y.M., Choi, N.T., Yang, Y., Gao, B.,
882 2017b. Wnt-induced Vangl2 phosphorylation is dose-dependently required for planar cell polarity in
883 mammalian development. *Cell Res.* 27, 1466–1484.

884 Yang, Y., Mlodzik, M., 2015. Wnt-Frizzled/planar cell polarity signaling: cellular orientation by facing the
885 wind (Wnt). *Annu. Rev. Cell Dev. Biol.* 31, 623–646.

886 Yates, L.L., Papakrivopoulou, J., Long, D.A., Goggolidou, P., Connolly, J.O., Woolf, A.S., Dean, C.H.,
887 2010a. The planar cell polarity gene Vangl2 is required for mammalian kidney-branching
888 morphogenesis and glomerular maturation. *Hum. Mol. Genet.* 19, 4663–4676.

889 Yates, L.L., Schnatwinkel, C., Hazelwood, L., Chessum, L., Paudyal, A., Hilton, H., Romero, M.R., Wilde,
890 J., Bogani, D., Sanderson, J., et al., 2013. Scribble is required for normal epithelial cell-cell contacts and
891 lumen morphogenesis in the mammalian lung. *Dev. Biol.* 373, 267–280.

892 Yates, L.L., Schnatwinkel, C., Murdoch, J.N., Bogani, D., Formstone, C.J., Townsend, S., Greenfield, A.,
893 Niswander, L.A., Dean, C.H., 2010b. The PCP genes *Celsr1* and *Vangl2* are required for normal lung
894 branching morphogenesis. *Hum. Mol. Genet.* 19, 2251–2267.

895 Ye, X., Wang, Y., Rattner, A., Nathans, J., 2011. Genetic mosaic analysis reveals a major role for frizzled 4
896 and frizzled 8 in controlling ureteric growth in the developing kidney. *Development* 138, 1161–1172.

897 Yu, H., Smallwood, P.M., Wang, Y., Vidaltamayo, R., Reed, R., Nathans, J., 2010. Frizzled 1 and frizzled 2
898 genes function in palate, ventricular septum and neural tube closure: general implications for tissue
899 fusion processes. *Development* 137, 3707–3717.

900 Yu, H., Ye, X., Guo, N., Nathans, J., 2012. Frizzled 2 and frizzled 7 function redundantly in convergent
901 extension and closure of the ventricular septum and palate: evidence for a network of interacting genes.
902 *Development* 139, 4383–4394.

903 Yuan, K., Shamskhou, E.A., Orcholski, M.E., Nathan, A., Reddy, S., Honda, H., Mani, V., Zeng, Y., Ozen,
904 M.O., Wang, L., et al., 2019. Loss of endothelium-derived Wnt5a is associated with reduced pericyte
905 recruitment and small vessel loss in pulmonary arterial hypertension. *Circulation* 139, 1710–1724.

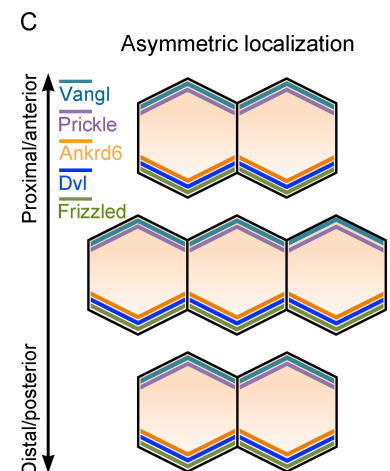
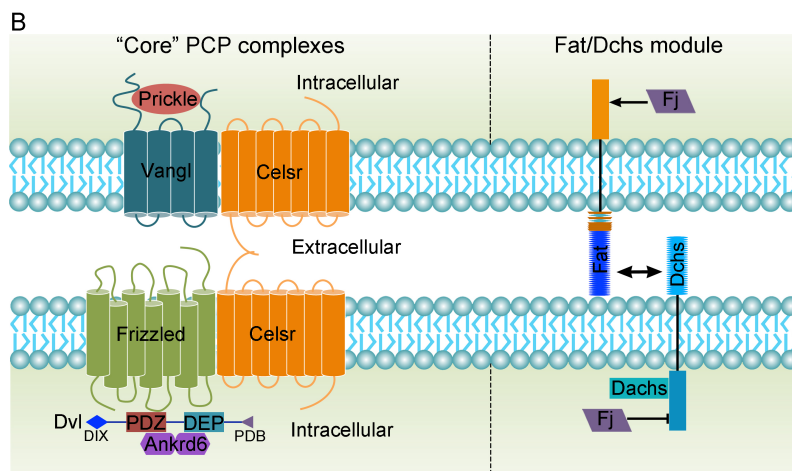
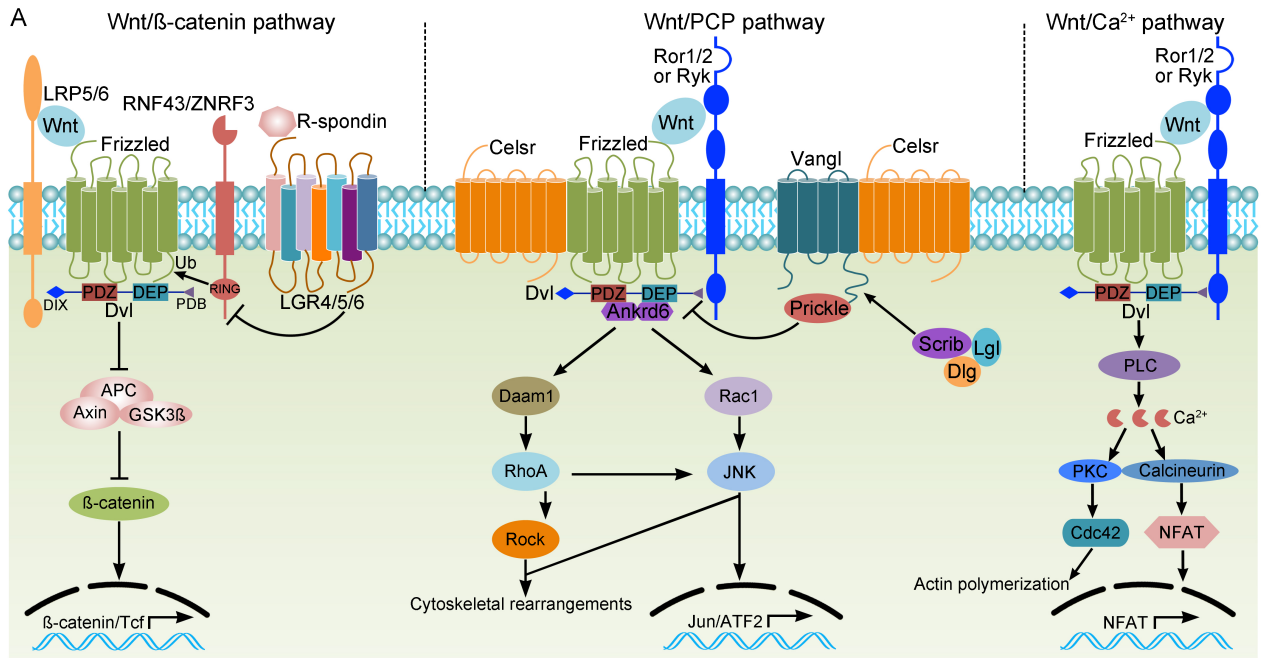
906 Yun, K., Ajima, R., Sharma, N., Costantini, F., Mackem, S., Lewandoski, M., Yamaguchi, T.P., Perantoni,
907 A.O., 2014. Non-canonical Wnt5a/Ror2 signaling regulates kidney morphogenesis by controlling
908 intermediate mesoderm extension. *Hum. Mol. Genet.* 23, 6807–6814.

909 Zhang, H., Bagherie-Lachidan, M., Badouel, C., Enderle, L., Peidis, P., Bremner, R., Kuure, S., Jain, S.,
910 McNeill, H., 2019. FAT4 fine-tunes kidney development by regulating RET signaling. *Dev. Cell* 48, 780–
911 792.e4.

912 Zhang, K., Yao, E., Lin, C., Chou, Y.T., Wong, J., Li, J., Wolters, P.J., Chuang, P.T., 2020. A mammalian
913 Wnt5a-Ror2-Vangl2 axis controls the cytoskeleton and confers cellular properties required for
914 alveologogenesis. *Elife* 9, e53688.

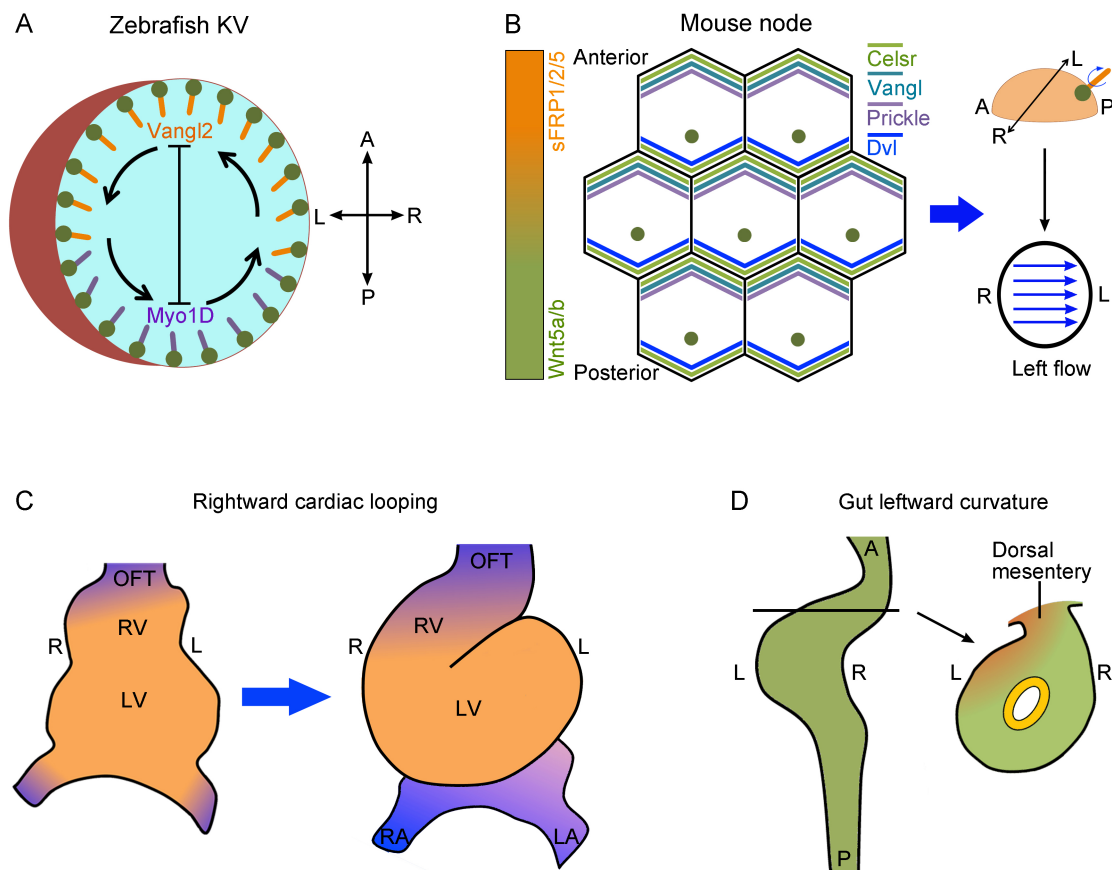
915 Zhou, W., Lin, L., Majumdar, A., Li, X., Zhang, X., Liu, W., Etheridge, L., Shi, Y., Martin, J., Van de Ven, W.,
916 et al., 2007. Modulation of morphogenesis by noncanonical Wnt signaling requires ATF/CREB family-
917 mediated transcriptional activation of TGFbeta2. *Nat. Genet.* 39, 1225–1234.

918



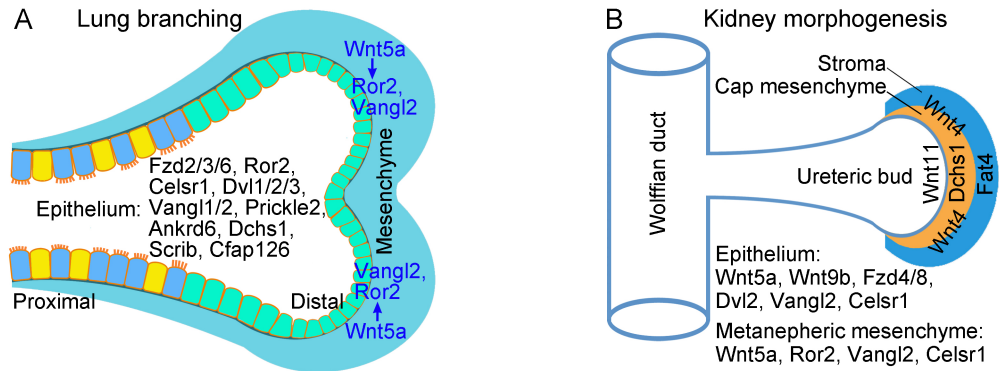
918
 919 **Fig. 1.** Wnt signaling branches and asymmetric localization of PCP protein complexes. **A:** Wnt/ β -
 920 catenin signaling is activated by ligands binding to Fzd receptors and LRP5/6 (low density
 921 lipoprotein receptor-related protein 5/6) co-receptors. The E3 RING ubiquitin ligases
 922 RNF43/ZNRF3 mediate the ubiquitination (Ub) of Fzd receptors for lysosomal degradation. This
 923 activity is inhibited by R-spondins binding to LGR4/5/6 (leucine-rich repeat containing G-protein
 924 coupled receptors). The Wnt/PCP pathway is induced by interaction of Wnts with the Fzd/Ror1/2
 925 (receptor tyrosine kinase-like orphan receptor 1/2) complex or the Fzd/Ryk (receptor tyrosine
 926 kinase) complex. The activation of downstream effectors leads to cytoskeletal rearrangements
 927 and/or transcription of ATF2 (activating transcription factor-2) target genes. The Scrib complex

928 can function to regulate Vangl asymmetric localization. The Wnt/Ca²⁺ branch triggers
 929 phospholipase C (PLC) activity through heteromeric G proteins to induce calcium-dependent
 930 responses. Dvl proteins mediate all Wnt signaling branches through distinct domains: N-terminal
 931 DIX, central PDZ, C-terminal DEP, and extreme C-terminus PDZ domain-binding (PDB) motif. **B:**
 932 The “core” PCP proteins function as two separately localized complexes, with Celsr forming
 933 homodimers between neighboring cells. Fat and Dchs form heterodimers between adjacent cells,
 934 acting as a ligand-receptor pair. Dachs is a Dchs-interacting unconventional myosin that functions
 935 as a key effector of Fat/Dchs signaling. **C:** Asymmetric subcellular localization of “core” PCP
 936 proteins along the proximal (anterior) and distal (posterior) axis in *Drosophila* epithelia.

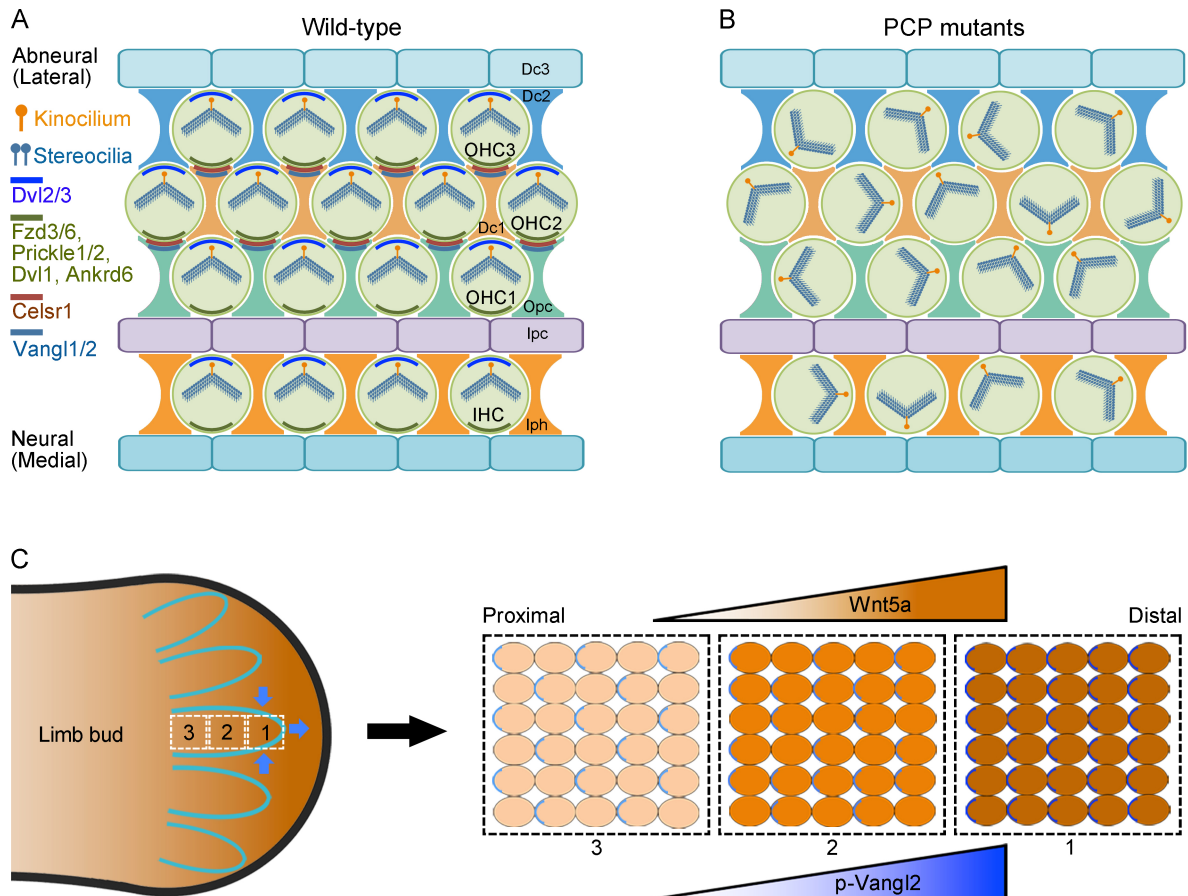


937
 938 **Fig. 2.** Left-right organizers and asymmetric organogenesis. **A:** In the zebrafish KV, Vangl2 and
 939 Myo1D coordinate leftward fluid flow (arrows) by regulating the localization of anteriorly (orange)
 940 and posteriorly (purple) pointing cilia. **B:** In the mouse node, Wnt5a/b gradients along the AP axis
 941 promote the asymmetric localization of PCP proteins. The posterior positioning of ciliary basal
 942 bodies (green dots) at the dome-shaped apical surfaces of node cells and the posterior tilting of

943 cilia generate leftward fluid flow within the node. **C:** Asymmetric heart morphogenesis. Ventral
 944 view shows rightward cardiac looping in E8.5-E9.5 mouse embryos. Progenitor cells derived from
 945 the SHF (blue) promote heart tube elongation, contributing to the development of OFT, right
 946 ventricule (RV) and the atria. RA, right atrium; LA, left atrium. **D:** Leftward curvature of gut tube.
 947 Transverse section at the horizontal line shows Wnt/PCP-mediated mesenchymal condensation
 948 (orange) on the left side of the dorsal mesentery in the chick embryo.



949
 950
 951 **Fig. 3.** PCP regulators in lung and kidney morphogenesis. **A:** At the earliest stage of lung
 952 branching morphogenesis in E10.5 mouse embryos, mesenchyme-derived Wnt5a activates the
 953 Ror2-Vangl2 cascade in the epithelium and mesenchyme to initiate distal lung morphogenesis.
 954 PCP proteins display asymmetric localization in bronchial epithelium composed of multiciliated
 955 cells and other cell types (yellow) as well as in distal lung epithelium. **B:** Schematic of ureteric
 956 bud development in E11 mouse embryos shows the interaction between the Wolffian duct-
 957 derived ureteric bud and its adjacent metanephric mesenchyme (stroma and cap mesenchyme).
 958 PCP proteins act in the mesenchyme and/or in the ureteric bud to promote ureteric bud
 959 branching, tubular elongation, and tubule diameter establishment. The Fat/Dchs polarity module
 960 mediates stroma-to-cap mesenchyme signaling in nephrogenesis.



961

962 **Fig. 4.** Wnt/PCP signaling in stereociliary bundle orientation and proximal-distal limb elongation.

963 **A:** In the organ of Corti, hair cells are aligned with supporting cells, including inner phalangeal

964 cells (Iph), inner pillar cells (Ipc), outer pillar cells (Opc), and Deiter cells (Dc1, Dc2, and Dc3).

965 The arrowhead-shaped hair bundles are uniformly oriented toward the abneural (lateral) edge of

966 the sensory epithelium. **B:** PCP mutants display mis-orientations of hair bundles, but each hair

967 cell still retains polarized stereocilia. Severe PCP phenotypes lead to strongly shortened and

968 thickened cochlea with additional rows of IHCs or OHCs. **C:** The graded expression of Wnt5a in

969 the developing limb bud provides global cues to establish a gradient of Vangl2 phosphorylation

970 and localization (blue) along the proximal-distal axis. Vangl2 induces polarized mesenchymal cell

971 behaviors toward the overlying ectoderm (black line), ensuring limb elongation and chondrocyte

972 differentiation. Circles in dashed boxes depict limb chondrocyte condensates expressing Wnt5a

973 and phosphorylated Vangl2. Wnt5a also generates anisotropic active stresses and controls CE

974 movements (blue arrows) to promote the formation of digit-organizing centers for digit

975 specification and elongation.

Table 1. Functions of PCP regulators in asymmetric organogenesis

Organs	PCP proteins	Functions	References
Left-right organizer	Wnt5a/b	Asymmetric localization of “core” PCP proteins in node cells	Minegishi et al., 2017
	Dvl2/3	Posterior positioning of ciliary basal bodies in node cells	Hashimoto et al., 2010
	Vangl1/2	Posterior tilting of primary motile cilia in node cells; posterior orientation of anteriorly positioned cilia in the zebrafish KV (Vangl2)	Borovina et al., 2010; Antic et al., 2010; Song et al., 2010; Juan et al., 2018
	Prickle1/2	Asymmetric distribution of microtubules and actomyosin networks for posterior positioning of ciliary basal bodies in node cells	Minegishi et al., 2017; Sai et al., 2022
	Prickle3	Basal body organization and cilia growth in <i>Xenopus</i> GRP	Chu et al., 2016
	Dchs1/2	Vangl1 localization and basal body positioning in node cells	Sai et al., 2022
	JNK1/2	Ciliogenesis and regulation of cilia length in the zebrafish KV	Derrick et al., 2022
Heart	Wnt5a/b	SHF deployment and AP elongation of the heart tube; OFT septation; polarization of actomyosin during heart tube remodeling (Wnt5b)	Sinha et al., 2015; Merks et al., 2018; Li et al., 2019
	Wnt11	OFT development and polarization of actomyosin networks during heart tube remodeling	Zhou et al., 2007; Merks et al., 2018
	Fzd4	Microtubule stabilization and cellular polarization during arterial and arteriolar formation	Descamps et al., 2012
	Fzd2/7	Redundantly involved in the closure of the ventricular septum	Yu et al., 2012
	Dvl1/2/3	SHF deployment and OFT lengthening	Sinha et al., 2012
	Vangl2	Polarized migration of myocardializing cells and OFT lengthening; formation of the coronary vasculature	Phillips et al., 2005, 2008; Ramsbottom et al., 2014

	Prickle1	Polarized cell orientations and intercalations for OFT lengthening	Gibbs et al., 2016
	Wdpcp	Polarized migration of cardiomyocytes to invade the OFT cushion	Cui et al., 2013
	Daam1/2	Cytoskeletal organization and cell adhesion for protrusion of cardiomyocytes into OFT	Li et al., 2011; Ajima et al., 2015
Gut	Wnt5a	Leftward tilt and gut elongation; re-intercalation of post-mitotic cells into gut epithelium and post-mitotic filopodial pathfinding in nuclear trafficking; chemoattractant for oriented migration of mesenchymal cells during villus formation; homeostatic renewal of adult intestinal epithelium	Cervantes et al., 2009; Matsuyama et al., 2009; Welsh et al., 2013; Wang et al., 2018; Shoshkes-Carmel et al., 2018; Dush and Nascone-Yoder, 2019; Rao-Bhatia et al., 2020
	Ror2	Midgut elongation (mesenchyme-derived Ror2 before phase I)	Wang et al., 2020
	Ryk	Midgut elongation by promoting post-mitotic filopodial pathfinding	Wang et al., 2020
	Vangl2	Oriented cell divisions to increase fore-stomach length; gut elongation and lumen formation; mesenchymal cell clustering in villus formation	Matsuyama et al., 2009; Dush and Nascone-Yoder, 2019; Rao-Bhatia et al., 2020
	Daam2	Mesenchymal condensation in the dorsal mesentery	Welsh et al., 2013
	Fat4/Dchs1	Mesenchymal cell clustering during villus formation	Rao-Bhatia et al., 2020
	Cfap126	Lineage priming and cell cycle exit at the base of the crypt for differentiation of Paneth and enteroendocrine cells	Böttcher et al., 2021
Lung	Wnt5a	Distal lung morphogenesis and lung maturation; alveologenesi; mesenchymal cell polarization for trachea and esophagus formation	Kishimoto et al., 2018; Li et al., 2020; Zhang et al., 2020
	Fzd2	Epithelial cell shape changes to promote branch point formation	Kadzic et al., 2014
	Fzd7	Pulmonary endothelium-pericyte interactions during pulmonary angiogenesis	Yuan et al., 2019
	Ror2	Pulmonary vasculogenesis; alveologenesi	Loscertales et al., 2008; Zhang et al., 2020
	Celsr1/Vangl2	Maintenance of epithelial architecture; branching morphogenesis;	Yates et al., 2010b; Li et al., 2020; Zhang et al.,

	alveologenesis	2020	
	Vangl1/Prickle2	Airway epithelial homeostasis and adult lung function	Vladar et al., 2016; Poobalasingam et al., 2017
	Scrib	Tight junction integrity and epithelial cohesion in lumen morphogenesis	Yates et al., 2013
	Cfap126	Diameter formation in terminal lung bronchioles	Gegg et al., 2014

	Wnt4	Mesenchymal to epithelial transformation for epithelialization of the ureteric bud	Stark et al., 1994; Kispert et al., 1998
	Wnt5a/Ror2	Metanephric mesenchyme positioning for interaction with the Wolffian duct; epithelial tubular formation from the ureteric bud	Nishita et al., 2014; Yun et al., 2014
	Wnt9b	CE movements and polarized cell divisions for tubular diameter formation	Karner et al., 2009
	Wnt11	Attachment of nephron progenitors to the epithelial tip for nephrogenic niche integrity	O'Brien et al., 2018
	Fzd4/8	Growth, branching and proliferation of the ureteric epithelium	Ye et al., 2011
	Dvl2	Rosette-based CE movements during kidney tubule elongation	Lienkamp et al., 2012
Kidney	Vangl1/2	Oriented cell divisions and CE movements in developing renal tubules; ureteric branching and glomerular maturation; organization of podocytes to protect glomerular injury in the adult (Vangl2)	Yates et al., 2010a; Rocque et al., 2015; Kunimoto et al., 2017
	Prickle1	Cell arrangements in the collecting duct and renal tubules	Liu et al., 2014
	Celsr1	Rostrocaudal patterning of renal tubules and maturation of glomeruli; promoting ureteric tree growth at early stages and inhibiting tubule overgrowth at late stages	Brzóska et al., 2016
	Fat1/Scrib	Cooperation with Fat4 in renal tubular elongation (Fat1); activation of Hippo signaling to regulate cell polarization and growth	Saburi et al., 2012; Skouloudaki et al., 2009
	Fat4/Dchs1	Oriented cell divisions for renal tubule elongation; Ureteric bud branching and tubule diameter formation; differentiation of ureteric epithelial	Saburi et al., 2008; Das et al., 2013; Mao et al., 2015; Bagherie-Lachidan et al., 2015; Zhang et

	progenitors; polarization of cap mesenchyme; inhibition of ectopic ureteric bud formation and kidney duplication (Fat4)	al., 2019
Daam1	Pronephric tubulogenesis; intercellular adhesion and epithelial tissue organization in CE and polarized movements	Miller et al., 2011; Krneta-Stankic et al., 2021
Fuz	Cilia-dependent and -independent ureteric bud branching	Wang et al., 2021
<hr/>		
Wnts	Cochlear extension and hair bundle orientation (interaction with Vangl2)	Najarro et al., 2020
Dvl1/2/3	Cochlear extension and hair bundle orientation	Montcouquiol et al., 2003; Wang et al., 2005
Wnt11/Fzd7	Alignment of support cells in zebrafish lateral line neuromasts	Navajas Acedo et al., 2019
Fzd1/2	Hair bundle orientation (interaction with Vangl2)	Yu et al., 2010
Fz3/6	Hair bundle orientation in the organ of Corti; cochlear innervation by type II spiral ganglion neurons	Wang et al., 2006; Ghimire and Deans, 2019
Vangl1/2	Cochlear extension and hair bundle orientation; post-natal organization of supporting cells to promote the function of OHCs (Vangl2); axon turning toward the cochlear base to innervate OHCs (Vangl2)	Montcouquiol et al., 2003; Wang et al., 2005; Copley et al., 2013; Ghimire et al., 2018
Inner ear		
Prickle1	Neurite growth of type II spiral ganglion neurons toward OHCs	Yang et al., 2017a
Celsr1	Earliest stages of hair cell polarity in the cochlea; hair bundle orientation in the vestibule associated with vestibular behaviors	Curtin et al., 2003; Duncan et al., 2017
Ankrd6	Hair bundle orientation in the utricle; polarity and patterning of hair cells in the cochlea (interaction with Vangl2)	Jones et al., 2014
Fat1/4	Cooperation in cochlear extension and patterning of OHCs	Saburi et al., 2012
PTK7	Hair bundle orientation in OHC3; functioning in supporting cells to exert polarized contractile tension on hair cells	Lu et al., 2004; Lee et al., 2012
Scrib	Planar polarization of stereociliary bundles (interaction with Vangl2)	Montcouquiol et al., 2003, 2006

	Cfap126	Kinocilium positioning and hair bundle morphogenesis in the cochlea	Gegg et al., 2014
	Wdpcp	Vangl2 asymmetric expression and kinocilium localization	Cui et al., 2013

	Wnt5a	Orientation of mesenchymal cell movements and divisions; chemoattractant for limb outgrowth; asymmetric localization and phosphorylation of Vangl2; generation of active stresses for the formation of digit-organizing centers	Yamaguchi et al., 1999; Gros et al., 2010; Wyngaarden et al., 2010; Gao et al., 2011; Parada et al., 2022
	Ror2	Phalange development and elongation through the digit-organizing center; phosphorylation of Vangl2	Witte et al., 2010; Gao et al., 2011
Limb bud	Dvl1/2/3	Interaction of casein kinase 1 with Vangl2 for Vangl2 phosphorylation	Yang et al., 2017b
	Vang2	Polarization of chondrocyte behaviors; elongation of proximal-distal axis; limb skeletal development	Gao et al., 2011; Wang et al., 2011
	Prickle1	Limb outgrowth; formation of distal skeletal elements; chondrocyte polarity and proximal-distal outgrowth of endochondral elements	Yang et al., 2013; Liu et al., 2014
	Ryk	Regulation of Vangl2 stability; interaction with Vangl2 in limb elongation	Andre et al., 2012